Neurobiology of Disease 134 (2020) 104665

Contents lists available at ScienceDirect

Neurobiology of Disease

journal homepage: www.elsevier.com/locate/ynbdi

Propranolol diminished severity of rat EAE by enhancing immunoregulatory/protective properties of spinal cord microglia

Ivan Pilipović[a], Zorica Stojić-Vukanić[b], Ivana Prijić[a], Nebojša Jasnić[c], Gordana Leposavić[d,*]

[a] Immunology Research Centre "Branislav Janković", Institute of Virology, Vaccines and Sera "Torlak", 458 Vojvode Stepe, 11221 Belgrade, Serbia
[b] Department of Microbiology and Immunology, University of Belgrade-Faculty of Pharmacy, 450 Vojvode Stepe, 11221 Belgrade, Serbia
[c] Institute for Physiology and Biochemistry, University of Belgrade-Faculty of Biology, Studentski trg 16, 11000 Belgrade, Serbia
[d] Department of Pathobiology, University of Belgrade-Faculty of Pharmacy, 450 Vojvode Stepe, 11221 Belgrade, Serbia

ARTICLE INFO

Keywords:
Experimental autoimmune encephalomyelitis
Noradrenaline
β-Adrenoceptor
Microglia
CX3CR1
Nrf2/HO-1 axis

ABSTRACT

Sympathetic dysfunction is suggested to contribute to development of multiple sclerosis and experimental autoimmune encephalomyelitis (EAE) alike. Considering important role of microglia in development/resolution of neuroinflammation, contribution of noradrenaline, the key sympathetic end-point mediator, in modulation of microglial phenotypic and functional properties in rat EAE model was examined. The study showed that noradrenaline acting in neurocrine and autocrine/paracrine way might influence microglia during EAE. Propranolol treatment over the effector phase moderated EAE course. This was associated with the increased proportion of microglia expressing CX3CR1, the key molecule in their immunomodulatory/neuroprotective action, and upregulation of CX3CR1 downstream Nrf2 gene. This correlated with the increased heme oxygenase-1 (HO-1) expression and phagocytic capacity of microglia, and their phenotypic changes mirrored in increased proportion of CD163- and CD83-expressing cells. The enhanced HO-1 expression was linked with the decreased proportion of microglial cells expressing IL-1β and IL-23, and possibly IL-6, followed by increased proportion of IL-10–expressing microglia, and downregulated MCP-1/CCL2 expression. Consistently, spinal cord infiltration with blood-borne myeloid and CD4+ T cells, as well as CD4+ T-cell reactivation/proliferation and differentiation into highly pathogenic IL-17+ cells co-producing IFN-γ and GM-CSF were decreased in propranolol-treated rats compared with saline-injected controls. The *in vitro* investigations of the effects of noradrenaline on microglia showed that noradrenaline through β-adrenoceptor may influence Nrf2 expression also via CX3CR1-independent route. The study suggests β-adrenoceptor–mediated neuroinflammation-promoting role of noradrenaline in EAE via modulation of microglial Nrf2 expression, and thereby forms the basis for further translational pharmacological research to improve multiple sclerosis therapy.

1. Introduction

Multiple sclerosis (MS) is the most common autoimmune disease of the central nervous system (CNS), which is pathohistologically characterized by inflammation and neurodegeneration causing a wide spectrum of clinical manifestations, including autonomic dysfunction (AD) (Lassmann and van Horssen, 2011). AD observed in 45% to 84% of MS patients leads to the fatigue, and various cardiovascular, bladder, bowel, ocular and sexual symptoms affecting quality of life of patients with MS (Flachenecker et al., 2003; Kodounis et al., 2005; Haensch and Jörg, 2006). AD in MS has been related to inflammation and demyelination in specific structures within the CNS (Polak et al., 2011). Among

Abbreviations: MS, multiple sclerosis; CNS, central nervous system; AD, autonomic dysfunction; EAE, experimental autoimmune encephalomyelitis; CD, cluster of differentiation; DA, Dark Agouti; d.p.i., day post immunization; PBS, phosphate-buffered saline; CFA, complete Freund's adjuvant; BW, body weight; RPMI, Roswell Park Memorial Institute; FCS, fetal calf serum; PMA, phorbol 12-myristate 13-acetate; IL, interleukin; MBP, myelin basic protein; LPS, lipopolysaccharide; ELISA, enzyme-linked immunosorbent assay; RT-qPCR, reverse transcription-quantitative polymerase chain reaction; HPLC, high performance liquid chromatography; HO-1, heme oxygenase-1; Nrf2, nuclear factor erythroid 2-related factor 2; iNOS, inducible nitric oxide synthase; Arg-1, arginase; MCP-1/CCL2, monocyte chemoattractant protein-1/C-C motif chemokine ligand 2; Ct, threshold cycle; Abs, antibodies; FITC, fluorescein isothiocyanate; PE, phycoerythrin; PerCP, peridinin-chlorophyll-protein; AF647, Alexa Fluor 647; APC, allophycocyanin; RT, room temperature; IFN, interferon; CX3CR1, C-X3-C motif chemokine receptor 1; GM-CSF, granulocyte monocyte colony-stimulating factor; MFI, mean fluorescence intensity; FMO, fluorescence minus one; ANOVA, analysis of variance; FKN, fractalkine

* Corresponding author.
E-mail address: gordana.leposavic@pharmacy.bg.ac.rs (G. Leposavić).

https://doi.org/10.1016/j.nbd.2019.104665
Received 5 August 2019; Received in revised form 8 October 2019; Accepted 30 October 2019
Available online 02 November 2019

these structures is locus coeruleus, a major noradrenaline source in the brain (whose activation, particularly during stress, leads to the sympathetic nervous system activation), and spinal cord (Haensch and Jörg, 2006; Polak et al., 2011). Additionally, AD is associated with altered catecholamine release from peripheral immune cells (Rajda et al., 2002). Specifically, higher adrenaline level in peripheral blood lymphocytes was found in first-attack MS patients than in healthy controls (Rajda et al., 2002). However, during remission in relapsing–remitting MS patients, noradrenaline levels in peripheral blood lymphocytes were lower than in healthy subjects (Rajda et al., 2002). Also, increased density of β-adrenoceptor on peripheral blood mononuclear cells from MS patients was reported (Karaszewski et al., 1990; Zoukos et al., 1992). Autonomic nervous system, particularly its sympatho-adrenomedullary branch, is the major pathway in the cross-talk between the CNS and the immune system (Elenkov et al., 2000; Nance and Sanders, 2007). Nevertheless, the significance of AD in the immunopathogenesis of MS has not yet been investigated in dedicated studies. Although target tissue critically determines autoimmune disease severity (Hill et al., 2007), data on β_2-adrenoceptor expression on CNS cells involved in imunopathogenesis of MS are limited. There are only a few reports pointing to astrocyte β_2-adrenoceptor deficiency in MS patients as a contributing factor to MS progression (Zeinstra et al., 2000; De Keyser et al., 2004).

Sympathetic/adrenergic dysregulation has also been observed in the development of experimental autoimmune encephalomyelitis (EAE) (del Rey et al., 1982; Mackenzie et al., 1989; Pilipović et al., 2019a), widely used group of experimental models mimicking various pathogenic and clinical aspects of MS (Robinson et al., 2014). Moreover, the role of β-adrenoceptor–mediated noradrenergic mechanisms in control of the primary immune responses in Dark Agouti (DA) rat EAE model has recently been described (Pilipović et al., 2019b). These data render the EAE model suitable for investigating the role of adrenergic mechanisms in development of MS.

EAE is characterized by an ascending paralysis resulting from spinal cord infiltration with neuroantigen-specific CD4+ T lymphocytes, major instigators/drivers of neuroinflammation in EAE (Shin et al., 2012), and inflammatory monocytes during the early stages of lesion development, followed by activation of microglia and neuronal and oligodendrocyte damage (Kim et al., 2007). Activated microglia, apart from the synthesis of proinflammatory mediators and promoting tissue damage upon the first wave of encephalitogenic T-cell immigration, may assume other functions (i.e. phagocytosis, anti-inflammatory mediator and growth factor release), to limit the CNS damage and promote tissue recovery (Sosa et al., 2013; Thompson and Tsirka, 2017). Thus, microglia are thought to be the key player in control of the autoimmune neuroinflammation in MS/EAE (Shin et al., 2012; Thompson and Tsirka, 2017). Although expression of β_2-adrenoceptor, the key adrenoceptor type involved in noradrenergic immunomodulation (Elenkov et al., 2000), on rodent spinal cord microglia (Tanaka et al., 2002; Hertz et al., 2010) and alterations in EAE rat spinal cord noradrenaline level (Leonard et al., 1990), have been revealed, there is no data on the role of noradrenaline in modulation of spinal cord inflammation and damage. However, substantial evidence obtained in unimmunized animals suggests that catecholamines may contribute to development of microglial proinflammatory phenotype (Walker et al., 2013; Frank et al., 2019).

Hereby reported study was undertaken to examine the putative β-adrenoceptor–mediated role of central noradrenaline in modulating neuroinflammation in EAE. In the first set of experiments, the influence of immunization for EAE on spinal cord noradrenaline level and β_2-adrenoceptor expression on microglia in DA rats was examined. In the second set of experiments, DA rats immunized for EAE (EAE rats) were treated with propranolol, a β-adrenoceptor antagonist crossing the blood-brain barrier (Neil-Dwyer et al., 1981), from the 8th day post immunization (d.p.i.) over the effector phase of EAE (Prop rats). Microglial cells and CD4+ T cells recovered from Prop rats and saline-injected controls (Sal rats) at the peak of EAE were examined for phenotypic and functional properties.

2. Materials and methods

2.1. Experimental animals

Three-month-old female DA rats were used in this study. The animals were bred in the animal facility of the Immunology Research Centre "Branislav Janković" and maintained under standard laboratory conditions (3 rats/cage, 12-h light/dark cycle, controlled temperature and humidity), with free access to rat chow and tap water. Animal health was monitored daily by the animal care staff and a veterinarian. All experimental procedures and animal care were in accordance with the Directive 2010/63/EU of the European Parliament and of the Council on the protection of animals used for scientific purposes. The study protocol was approved by the Ethical Committees of the Institution and of the Republic of Serbia (Ministry of Agriculture, Forestry and Water Economy of the Republic of Serbia - Veterinary Directorate; permit no. 323-07-01577/2016-05/14). All experiments complied with ARRIVE guidelines for reporting animal research.

2.2. Induction and clinical evaluation of EAE

For EAE induction, 100 µl of emulsion comprising equal volumes of rat spinal cord homogenate in phosphate-buffered saline (PBS) and complete Freund's adjuvant (CFA) containing 1 mg/ml of heat-killed and dried *Mycobacterium tuberculosis* H37Ra (Sigma-Aldrich Chemie GmbH, Taufkirchen, Germany) was administered, followed by a subcutaneous injection of 5×10^8 *Bordetella pertussis* (Institute "Torlak", Belgrade, Serbia) saline suspension, as previously described in detail (Nacka-Aleksić et al., 2015). To minimize animal suffering, the rats were anesthetized before immunization using an intraperitoneal injection of 50 mg/kg body weight (BW) of ketamine (Ketamidor, Richter Pharma AG, Wels, Austria; 100 mg/ml) and 5 mg/kg BW of xylazine (Xylased, Bioveta, Ivanovice na Hané, Czech Republic; 20 mg/ml). Starting from the 1st d.p.i., the animals were daily monitored for neurological deficit by two experienced independent observers: 0, no clinical signs; 0.5, distal tail atony; 1, complete tail atony; 2, paraparesis; 3, paraplegia; 4, tetraplegia or moribund state. Facilitated access to mashed food and water was provided for all the animals which exhibited clinical signs of EAE. Rats were sacrificed through transcardial perfusion, following the deep anesthesia induced by intraperitoneal injection of ketamine/xylazine cocktail (80 mg/kg BW/8 mg/kg BW).

2.3. Experimental design

Two sets of experiments were performed. In the first set of experiments, spinal cords of EAE rats and non-immunized controls were examined for either (i) tissue noradrenaline level and tyrosine hydroxylase mRNA expression, or (ii) microglial β_2-adrenoceptor expression and microglial/CD4+ T-cell tyrosine hydroxylase expression. EAE rats were sacrificed in the inductive phase and at the peak of the disease, on the 8th and the 14th d.p.i., respectively. Six rats per group per experiment were used. The second set of experiments was initiated by a preliminary study examining the effects of non-selective β-AR antagonist propranolol treatment over the effector phase of EAE on the clinical picture of the disease. Starting from the 8th d.p.i., rats were subcutaneously administered with 10 mg/kg of propranolol [(±)-propranolol hydrochloride; Sigma-Aldrich Chemie GmbH] or saline twice daily, and monitored for clinical signs of EAE until the full recovery (9 rats per group). Aside from capacity to block all β-AR receptors without toxic effects (Robinson et al., 2011), the dose of propranolol was selected considering our previous study suggesting that it may act at the spinal cord level to influence clinical EAE development in DA rats (Pilipović et al., 2019b). Follow-up experiment was performed to

elucidate cellular/molecular mechanisms of propranolol action on clinical EAE, by assessing phenotypic/functional properties of spinal cord microglia and infiltrating CD4+ T cells recovered at the peak of EAE from Prop and Sal rats (6 rats per group). Additionally, *in vitro* effects of noradrenaline and/or propranolol on spinal cord microglia were examined in an experiment encompassing 6 rats sacrificed at the peak of EAE.

2.4. Isolation of mononuclear cells

Following perfusion, spinal cords were removed and dissociated on a 70-μm nylon cell strainer (BD Biosciences, Erembodegem, Belgium) in ice-cold RPMI 1640 medium (Sigma-Aldrich Chemie GmbH) containing 5% fetal calf serum (FCS; Capricorn Scientific GmbH, Ebsdorfergrund, Germany). Spinal cord single-cell suspensions were then further fractioned on a discontinuous 40/70% Percoll (Sigma-Aldrich Chemie GmbH) gradient at 1000 g for 50 min. The cells collected from the interface were enumerated using Neubauer chamber and 0.2% trypan blue dye to exclude non-viable cells.

2.5. Mononuclear cell cultures

All cultures were set up using complete RPMI 1640 medium containing 2 mM L-glutamine (Serva, Heidelberg, Germany), 1 mM sodium pyruvate (Serva), penicillin (100 units/ml)/streptomycin (100 μg/ml) solution (Sigma-Aldrich Chemie GmbH), 50 μM β-mercaptoethanol and 10% FCS. For analyses of *in vitro* effects of noradrenaline (arterenol) and/or propranolol, the medium was further supplemented with 100 μM of ascorbic acid. The cells were cultivated at a density of 10^6/ml, in a 5% CO_2 humidified atmosphere at 37 °C.

2.5.1. Restimulation for intracellular cytokine staining

For intracellular cytokine staining, freshly isolated cells were restimulated for 4 h with 200 ng/ml of phorbol 12-myristate 13-acetate (PMA, Sigma-Aldrich Chemie GmbH) and 400 ng/ml ionomycin (Sigma-Aldrich Chemie GmbH) in the presence of 3 μg/ml of brefeldin A (eBioscience).

For assessing neuroantigen-specific production of IL-17, to the cells cultured overnight in the absence or in the presence of 20 μg/ml of myelin basic protein (MBP, Sigma-Aldrich Chemie GmbH) (recall test), brefeldin A was added for the last 4 h of culture.

2.5.2. Assessment of noradrenaline and/or propranolol effects on microglia in culture

Cells from EAE rats were incubated in the RPMI 1640 medium alone or pretreated with 10^{-6} M of arterenol [(±)-noradrenaline(+)-bitartrate salt, Sigma-Aldrich Chemie GmbH] for 1 h, or 10^{-5} M of propranolol for 15 min. When both antagonist and agonist were used, arterenol was added 15 min after propranolol. The dose of arterenol was chosen considering that (i) supraphysiological (i.e. $\geq 10^{-6}$ M) noradrenaline concentrations are required for functional changes in immune cells *in vitro* (Padro and Sanders, 2014), and (ii) 10^{-6} M of noradrenaline effectively modulates rat microglial functions (Tanaka et al., 2002). Following pretreatment, the cells were either (i) assayed for phagocytosis, or (ii) stimulated overnight with 1 μg/ml of lipopolysaccharide (LPS; Sigma-Aldrich Chemie GmbH) for measurements of supernatant cytokine concentrations by enzyme-linked immunosorbent assay (ELISA), or cell gene expression analysis by reverse transcription-quantitative polymerase chain reaction (RT-qPCR).

2.6. Noradrenaline measurement

For high performance liquid chromatography (HPLC) analysis, spinal cords were snap-frozen in liquid nitrogen and immediately stored at −70 °C. Tissue samples were homogenized in DEPROT solution (1 mg: 20 μl) containing 2% ethylene glycol tetraacetic acid, 0.1 N $HClO_4$ and 0.2% $MgCl_2$, then sonicated and centrifuged (30 min, 18,000 rpm, +4 °C). Collected supernatants were injected with the autosampler of a Dionex UltiMate 3000 HPLC system (Thermo Scientific, Sunnyvale, CA, USA) equipped with a Hibar 125–4 LiCrospher100 RP-18 (5 μm) HPLC column (Merck Millipore, Darmstadt, Germany). Chromeleon7 Chromatography Data System (Thermo Scientific) was used for instrument control and data acquisition. The mobile phase consisted of 98% ammonium formate buffer (Fisher Scientific, Cambridge, UK, pH 3.6) and 2% methanol (J.T.Baker, Griesheim, Germany) and its flow rate was set at 500 μl/min. The potential for electrochemical measurements was set at +850 mV and the separation temperature at 25 °C. Noradrenaline standard solutions (DL-noradrenaline hydrochloride) were made from the stock standard solution (1 mg/ml of noradrenaline in methanol) in DEPROT, with concentration range 0.5–25 μg/ml. If not stated otherwise, all the chemicals were provided by Sigma-Aldrich Chemie GmbH.

2.7. RT-qPCR

Snap-frozen spinal cord tissue samples and mononuclear cells lysed/homogenized in TRIzol extraction reagent (Invitrogen Life Technologies, Carlsbad, CA, USA) were stored at −70 °C until RNA purification. Total RNA extraction was performed using TRIzol reagent according to the manufacturer's instructions. The RNA concentration and purity were determined by spectrophotometric analysis (OrionTM AquaMate 8000 from Thermo Scientific, Waltham, MA, USA). For cDNA synthesis, a High Capacity cDNA Reverse Transcription Kit (Applied Biosystems) was used, as suggested by the manufacturer. RT-qPCR reaction mixtures contained 5 μl of cDNA template, 1× TaqMan Gene Expression Master Mix with Uracil-DNA glycosylase (UDG) (Applied Biosystems) and 1× mix of premade primer and hydrolysis probe sets (TaqMan Gene Expression Assays, Applied Biosystems) in a total volume of 25 μl. Reactions in triplicate were performed under the default Applied Biosystems 7500 Real-Time PCR System conditions. TaqMan Gene Expression Assays detailed in Supplementary Table 1 were used to analyze the expression of tyrosine hydroxylase, IL-6, heme oxygenase-1 (HO-1), nuclear factor erythroid 2-related factor 2 (herein referred to as Nrf2), inducible nitric oxide synthase (iNOS), arginase 1 (Arg-1), monocyte chemoattractant protein-1/C-C motif chemokine ligand 2 (MCP-1/CCL2) and β-actin. Target mRNA expression was assessed using the SDS v1.4.0. software (Applied Biosystems) and comparative threshold cycle (dCt) method, with β-actin as a reference gene. The difference between threshold cycle values of the target and reference gene (dCT = Ct target – Ct reference) in each sample was calculated and the target gene expression relative to the reference gene was expressed as 2^{-dCt} value. The ratio of iNOS to Arg-1 expression was calculated as follows: 2^{-dCt} iNOS/2^{-dCt} Arg-1 (Brown et al., 2009).

2.8. Flow cytometry analysis

2.8.1. Antibodies and immunoconjugates

For immunolabeling, the following antibodies (Abs) and second step reagents (detailed in Supplementary Table 2) were used according to maufacturers' instructions. Unconjugated anti-tyrosine hydroxylase from EMD Millipore (Billerica, MA, USA). Unconjugated anti-β_2-adrenoceptor (H-73), unconjugated anti-CD83 (N-15) and phycoerythrin (PE)-conjugated donkey anti-goat IgG from Santa Cruz Biotechnology (Dallas, TX, USA). Fluorescein isothiocyanate (FITC)-conjugated anti-CD11b and PE-conjugated anti-CD45 from Serotec (Oxford, UK). Biotin-conjugated anti-CD45, biotin-conjugated anti CD11b, PE-conjugated anti-ED2 (CD163), PE-conjugated anti-IL-10, FITC/PE-conjugated anti-CD4, peridinin-chlorophyll-protein (PerCP)-conjugated anti-TCRαβ, PE-conjugated anti-IL17A, FITC-conjugated anti-IFN-γ, FITC-conjugated goat anti-rabbit IgG, PE-conjugated F(ab')2 donkey anti-rabbit IgG and PE-conjugated anti-Ki-67 from BD Biosciences Pharmingen (Mountain View, CA, USA). Unconjugated anti-CX3CR1 from Abcam

(Cambridge, UK) and unconjugated anti-IL-23 from Bioss (Woburn, MA, USA). Alexa Fluor 647 (AF647)-conjugated anti-TCRαβ and PerCP-conjugated streptavidin from BioLegend (San Diego, CA, USA). FITC-conjugated anti-Foxp3, allophycocyanin-conjugated anti-CD4 and PerCP-eFluor 710-conjugated anti-CD25 from eBioscience (San Diego, CA, USA). AF647-conjugated anti-GM-CSF and unconjugated anti-IL-1β from Novus Biologicals (Littleton, CO, USA).

2.8.2. Surface and intracellular antigen immunolabeling

Aliquots of freshly isolated cells (for surface antigen immunostaining) or cells fixed/permeabilized for intracellular antigen immunostaining according to eBioscience protocol (http://www.ebioscience.com/resources/best-protocols/flow-cytometry-protocols.htm) were incubated with saturating concentrations of fluorochrome-labeled Abs or biotin-conjugated/unconjugated Abs (30 min, 4 °C, if not stated otherwise). When biotin-conjugated/unconjugated Abs were used, the cells were washed following the incubation and the appropriate second step reagents were applied. Immunolabeling of intracellular cytokines was carried out at room temperature (RT).

To determine cell apoptosis, after labeling of the surface markers, spinal cord cells were washed with PBS and then with 1× Annexin V binding buffer (BD Bisciences Pharmingen). The cells were then incubated with Annexin V-FITC (BD Biosciences Pharmingen) for 15 min at RT and collected for flow cytometry analysis.

2.8.3. Phagocytosis of latex beads

Yellow-green fluorescent carboxylated polystyrene latex beads used for phagocytosis assay (1 μm diameter, Sigma-Aldrich Chemie GmbH) were sonicated in an ultrasound bath for 2 min at RT. Spinal cord cells were incubated with latex beads (bead:cell ratio of 50:1) for 1 h at 37 °C in complete RPMI 1640 medium with 5% FCS. To arrest the phagocytosis, the cells were incubated on ice for 5–10 min and after washing in ice-cold PBS, subjected to surface antigen immunostaining. Cells incubated at 4 °C were used to determine the positive/negative cut-off for latex-containing (Latex+) cells in flow cytometry analysis.

2.8.4. Endocytosis of FITC-dextran

Spinal cord cells were incubated in complete RPMI 1640 medium with 5% FCS containing 1 mg/ml FITC-conjugated dextran (Sigma-Aldrich Chemie GmbH) for 90 min at 37 °C. Excess dextran was removed by washing the cells in ice-cold PBS supplemented with 2% FCS and 0.1% NaN_3 and the cells were stained for surface antigens. Cells incubated at 4 °C were used to determine the positive/negative cut-off for dextran-containing (Dextran+) cells in flow cytometry analysis.

2.8.5. Data acquisition and analysis

For analyses, 50,000 events per sample were acquired on FACSVerse or FACSCalibur flow cytometer (Becton Dickinson, Mountain View, CA, USA). FlowJo software version 7.8. (TreeStar Inc., Ashland, OR, USA) was used to determine the frequency of marker positive cells and/or mean fluorescence intensity (MFI), expressed as MFI ratio (MFI of antibody-labeled cells/MFI of unstained negative control cells) (Reguzzoni et al., 2002), which is indicative of the antigen expression level. Fluorescence minus one (FMO)/isotype controls were used to set the gating boundaries, except for markers exhibiting clear bimodal staining (Alvarez et al., 2010).

2.9. ELISA cytokine measurement

Commercially available ELISA kits were used to determine the concentrations of secreted IL-1β (Thermo Fisher Scientific Inc., Rockford, IL, USA) and IL-10 (R&D Systems, Minneapolis, MN, USA) in cell-free culture supernatants. Measurements were performed according to the manufacturers' instructions, with detection sensitivity of ≤12 pg/ml for IL-1β and < 10 pg/ml for IL-10.

2.10. Statistical analysis

Statistical analyses were performed using GraphPad Prism Software (version 5.00; GraphPad Software, San Diego, CA, USA). The effects of *in vivo* propranolol treatment were assessed using unpaired Student's *t*-test, unless indicated otherwise. The influence of immunization for EAE on the examined parameters was evaluated using one-way analysis of variance (ANOVA), while *in vitro* effects of arterenol/propranolol were analyzed by repeated measures one-way ANOVA. Tukey test was used for the *post-hoc* comparisons. The results were presented as mean ± SEM. Values of $p \leq .05$ were considered significant.

3. Results

3.1. The first set of experiments: spinal cord noradrenaline level and β_2-adrenoceptor expression on microglia during EAE development

The first set of experiments was designed based on data showing β_2-adrenoceptor–mediated immunomodulatory properties of noradrenaline (Elenkov et al., 2000), and significance of the target organ microenvironment for the clinical outcome of EAE (Kawakami et al., 2004). Noradrenaline level in spinal cord and β_2-adrenoceptor expression on microglia were examined.

3.1.1. Different changes in spinal cord noradrenaline level and tyrosine hydroxylase expression in microglia during EAE development

The level of noradrenaline in spinal cord changed with EAE development. On the 8th d.p.i., noradrenaline level in spinal cord of EAE rats was comparable to that in control non-immunized rats (Fig. 1A). However, on the 14th d.p.i., it was lower ($p < .05$) than in non-immunized animals (Fig. 1A). Consistently, spinal cord expression of mRNA for tyrosine hydroxylase, the enzyme catalyzing the rate-limiting step in catecholamine biosynthesis (Flatmark, 2000), exhibited similar pattern of changes to that observed in noradrenaline level during EAE development (Fig. 1A). Next, considering recent data indicating that intrinsic myeloid cell synthesis of catecholamines serves to amplify inflammatory cascades in these cells (Staedtke et al., 2018), tyrosine hydroxylase expression in microglia was examined. Microglia were identified as CD11b+CD45$^{lo/int}$ cells (Almolda et al., 2009) and examined using flow cytometry analysis. The gating boundary between CD11b+CD45$^{lo/int}$ and CD11b+CD45^{hi} cells was settled by analyzing CD11b/CD45 expression on spinal cord cells recovered from non-immunized control rats (Fig. 1B), as previously suggested (Djikić et al., 2014). On the 8th and 14th d.p.i., both the frequency of tyrosine hydroxylase+ cells and density of tyrosine hydroxylase expression in these cells (judging by tyrosine hydroxylase MFI) were higher ($p < .01$) in EAE rats compared with non-immunized controls (Fig. 1C). Thus, it is clear that the decrease in spinal cord noradrenaline level and tyrosine hydroxylase expression during the course of EAE could not be ascribed to the changes in microglia.

3.1.2. Changes in β_2-adrenoceptor expression on microglia during EAE development

Next, the expression of β_2-adrenoceptor on microglia was examined to assess putative functional implications of the immunization-induced changes in spinal cord noradrenaline level. Flow cytometry analysis showed that CD11b+CD45$^{lo/int}$ microglia from both EAE rats and non-immunized controls bear surface β_2-adrenoceptor. On the 8th d.p.i., their frequency within spinal cord CD11b+CD45$^{lo/int}$ cells and the density of β_2-adrenoceptor on their surface (judging by β_2-adrenopceptor MFI) were comparable to those in non-immunized controls (Fig. 1D). Differently, on the 14th d.p.i., at the peak of the disease, both the frequency of β_2-adrenoceptor+ cells within spinal cord CD11b+CD45$^{lo/int}$ cells and its surface density on these cells exceeded ($p < .001$) the values detected in controls (Fig. 1D).

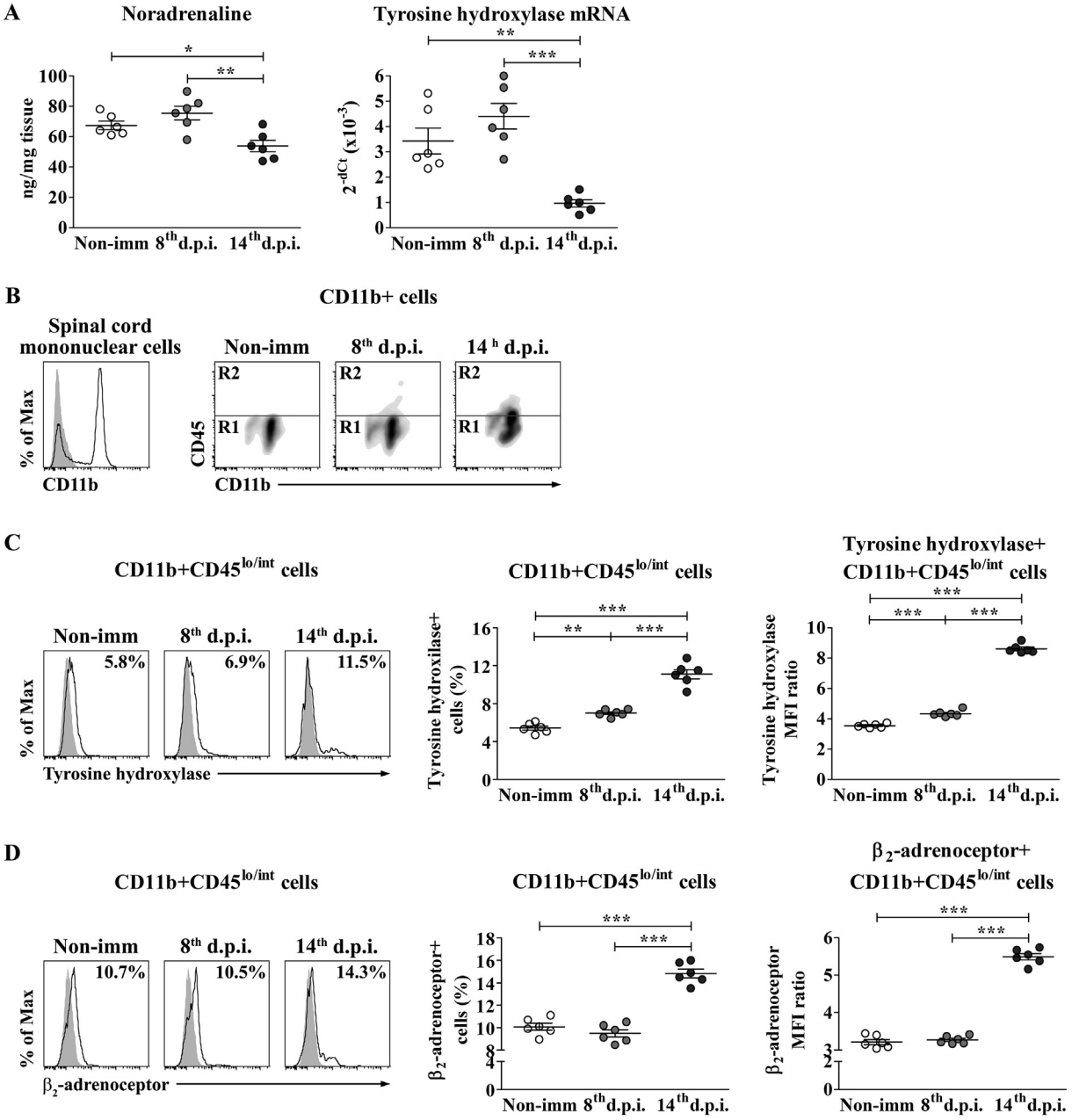

Fig. 1. Changes in spinal cord noradrenaline concentration and microglial tyrosine hydroxylase/β_2-adrenoceptor expression during EAE development. **(A)** Scatter plots indicate (left) noradrenaline concentration and (right) tyrosine hydroxylase mRNA expression in spinal cord tissue samples retrieved from rats immunized for EAE (EAE rats) on the 14th and the 8th d.p.i., or non-immunized control animals (Non-imm). Relative mRNA expression levels were determined by RT-qPCR and shown as 2^{-dCt} value relative to β-actin. (**B**) Flow cytometry density plots indicate CD45 immunostaining of CD11b+ spinal cord cells retrieved from EAE rats at distinct stages of the disease and non-immunized control animals. The gating boundary between CD11b+CD45$^{lo/int}$ (R1 region) and CD11b+CD45^{hi} cells (R2 region) was settled based on (left density plot) CD11b vs CD45 immunostaining of spinal cord cells from non-immunized healthy rats. Black flow cytometry histogram indicates the gating strategy for CD11b+ cells, based on (shaded histogram) FMO control incubated with isotype control antibody (Ab) instead of anti-CD11b Ab. **(C, D)** Black flow cytometry histograms indicate the frequencies of **(C)** tyrosine hydroxylase+ and **(D)** β_2-adrenoceptor+ cells among spinal cord CD11b+CD45$^{lo/int}$ microglia retrieved from EAE rats at distinct stages of the disease and non-immunized control animals. The gating boundaries for **(C)** tyrosine hydroxylase+ and **(D)** β_2-adrenoceptor+ cells were settled using (shaded histograms) FMO controls without corresponding primary Abs, incubated with secondary Abs alone. Scatter plots indicate (left) the frequency of **(C)** tyrosine hydroxylase+ and **(D)** β_2-adrenoceptor+ cells among CD11b+CD45$^{lo/int}$ microglia, and (right) **(C)** tyrosine hydroxylase and **(D)** β_2-adrenoceptor MFI in/on the corresponding cells from EAE rats at distinct stages of the disease and non-immunized control animals. The data are shown as mean ± SEM (n = 6 rats/group). Horizontal bars in scatter plots indicate mean values. * $p \leq .05$; ** $p \leq .01$; *** $p \leq .001$.

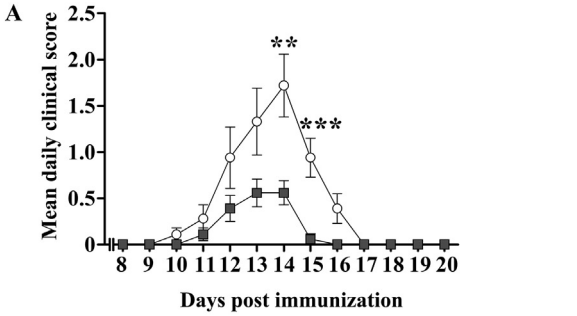

	Disease duration	Maximum neurological score	Clinical severity index
Sal	4.7±0.55	1.8±0.37	1.1±0.17
Prop	2.3±0.52*	0.81±0.09*	0.56±0.08*

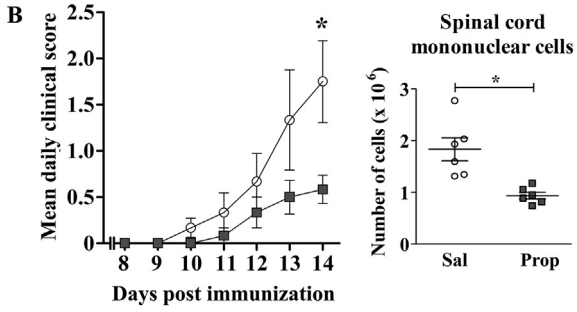

Fig. 2. Propranolol treatment over the effector phase of EAE decreases the severity of the disease and spinal cord-infiltrating cell number. (A) Line graph indicates the mean daily clinical score of EAE in rats treated with propranolol (Prop) or administered with saline (Sal) over the effector phase of the disease starting from the 8th d.p.i. until the full recovery, as shown in a preliminary experiment. The disease duration (days), maximum neurological score (the sum of the highest clinical scores/number of rats with clinical EAE) and clinical severity index (the cumulative clinical score/the number of days with clinical EAE) are given in the table. The data are shown as mean ± SEM (n = 9 rats/group). * p ≤ .05; ** p ≤ .01; *** p ≤ .001. **(B)** Line graph indicates the mean daily clinical score of EAE in Prop and Sal rats, sacrificed on the 14th d.p.i. in a follow-up experiment examining the number and phenotypic/functional properties of spinal cord cells. Scatter plot indicates the number of spinal cord mononuclear cells retrieved from these animals. The data are shown as mean ± SEM (n = 6 rats/group). Horizontal bars in scatter plot indicate mean values. * $p \leq .05$. Except for the disease duration and spinal cord mononuclear cell number, Mann-Whitney *U* test was used for statistical analysis.

3.2. The second set of experiments: influence of propranolol treatment during the effector phase of EAE on clinical manifestations of the disease and underlying immunopathogenic mechanisms

3.2.1. Propranolol administration over the effector phase of EAE decreases the severity of the disease and reduces the number of mononuclear cells retrieved from spinal cord at the peak of the disease

In the second set of experiments, the influence of propranolol treatment over the effector phase of EAE on the clinical manifestations of the disease was investigated. Prop rats, as Sal controls, developed acute monophasic disease reaching the peak between the 13th and the 14th d.p.i. (Fig. 2A). Prop rats developed milder disease than Sal animals, judging by lower ($p < .05$) mean maximum neurological score (Fig. 2A). Additionally, shorter ($p < .05$) duration of the clinical disease and decreased ($p < .05$) clinical severity index (i.e. cumulative clinical score of each rat divided by the number of days with clinical EAE) were found in Prop rats than in Sal ones (Fig. 2A).

In the second experiment, which was settled to examine the influence of propranolol on immunological parameters, similar clinical picture of EAE was observed. Spinal cord mononuclear cells recovered at the peak of EAE were examined for the number and phenotypic and functional properties. In accordance with milder disease, fewer ($p < .05$) mononuclear cells were retrieved from spinal cord of Prop rats compared with Sal controls (Fig. 2B).

3.2.2. Propranolol increases the frequency of CX3CR1-expressing microglial cells and proportion of microglia with immuoregulatory/protective properties in spinal cord at the peak of EAE

Next, the effects of propranolol on phenotypic and functional properties of spinal cord microglia were examined. Given that signaling mediated through C-X3-C motif chemokine receptor 1 (CX3CR1), unique receptor for fractalkine (FKN, formally known as CX3CL1), expressed on microglia has the crucial role in limiting neuroinflammation (Wolf et al., 2013), CX3CR1 surface expression on microglia was examined. Prop rats exhibited higher ($p < .001$) frequency of CX3CR1+ cells among microglia than Sal controls (Fig. 3A). Additionally, greater ($p < .001$) density of CX3CR1 was found on microglia from Prop rats compared with Sal rats (Fig. 3A). Given that CX3CR1-mediated signaling is shown to be the key regulator of the Nrf2 transcription factor expression (Lastres-Becker et al., 2014), Nrf2 mRNA expression level in spinal cord cells was also investigated. Indeed, greater ($p < .001$) amount of Nrf2 mRNA was found in spinal cord cells of Prop rats compared with Sal controls (Fig. 3B).

Given that Nrf2 stimulates the expression of TAM (Tyro3, Axl, and Mertk) receptors (Castro-Sánchez et al., 2019) essential in regulation of phagocytosis (Ji et al., 2015), microglial cells were examined for phagocytosis of fluorescent latex beads. The frequency of Latex+ cells was higher ($p < .001$) among microglia from Prop rats compared with Sal controls (Fig. 3C). Considering that noradrenaline via β-adrenoceptor may affect phagocytosis without affecting CX3CL1/CX3CR1 axis (Rossi et al., 1998), and that CX3CL1 expression is confined to certain neurons, but not to mononuclear cells (Wolf et al., 2013), the influence of noradrenaline (arterenol) on phagocytic capacity of microglial cells from EAE rat spinal cord mononuclear cell cultures was also examined. Compared with spinal cord mononuclear cell cultures grown in the medium alone (Control), in arterenol-supplemented cultures the frequency of Latex+ cells among microglia ($p < .001$) was decreased (Fig. 3D). In the co-presence of propranolol, arterenol was inefficient in this respect (Fig. 3D). Notably, the frequency of Latex+ cells among microglia from spinal cord mononuclear cell cultures was increased ($p < .01$) in the presence of propranolol alone (Fig. 3D), supporting catecholamine production by immune cells (Laukova et al., 2013; Staedtke et al., 2018; Pilipović et al., 2019a).

To assess if this effect of arterenol involves Nrf2, the expression of its transcript in LPS-stimulated spinal cord mononuclear cell cultures (LPS cultures) supplemented with arterenol and/or propranolol was explored. In the presence of LPS, Nrf2 mRNA expression was downregulated ($p < .05$) compared with that in control cultures with medium alone (Fig. 3E). In arterenol-supplemented LPS cultures, Nrf2 mRNA expression was decreased ($p < .001$) compared with those with LPS alone (Fig. 3E). In the co-presence of propranolol, arterenol did not significantly influence Nrf2 mRNA expression (Fig. 3E). Thus, it may be assumed that noradrenaline influences Nrf2 expression in both CX3CR1-dependent and CX3CR1-independent manner.

Given that the expression of CD163 on microglia is associated with phagocytosis of cellular debris and apoptotic/necrotic cells (Zhang et al., 2011), its expression on microglial cells was examined as well. The frequency of CD163+ cells among CD11b+CD45$^{lo/int}$ microglial cells, and the density of CD163 on their surface, were greater ($p < .001$) in Prop rats than in Sal controls (Fig. 4A). Given that CD163-expressing cells are shown to be alternatively activated cells expressing the mannose receptor (Mammana et al., 2018), microglia was assayed for mannose receptor-dependent endocytosis of dextran. Indeed, the frequency of Dextran+ cells was higher ($p < .001$) among

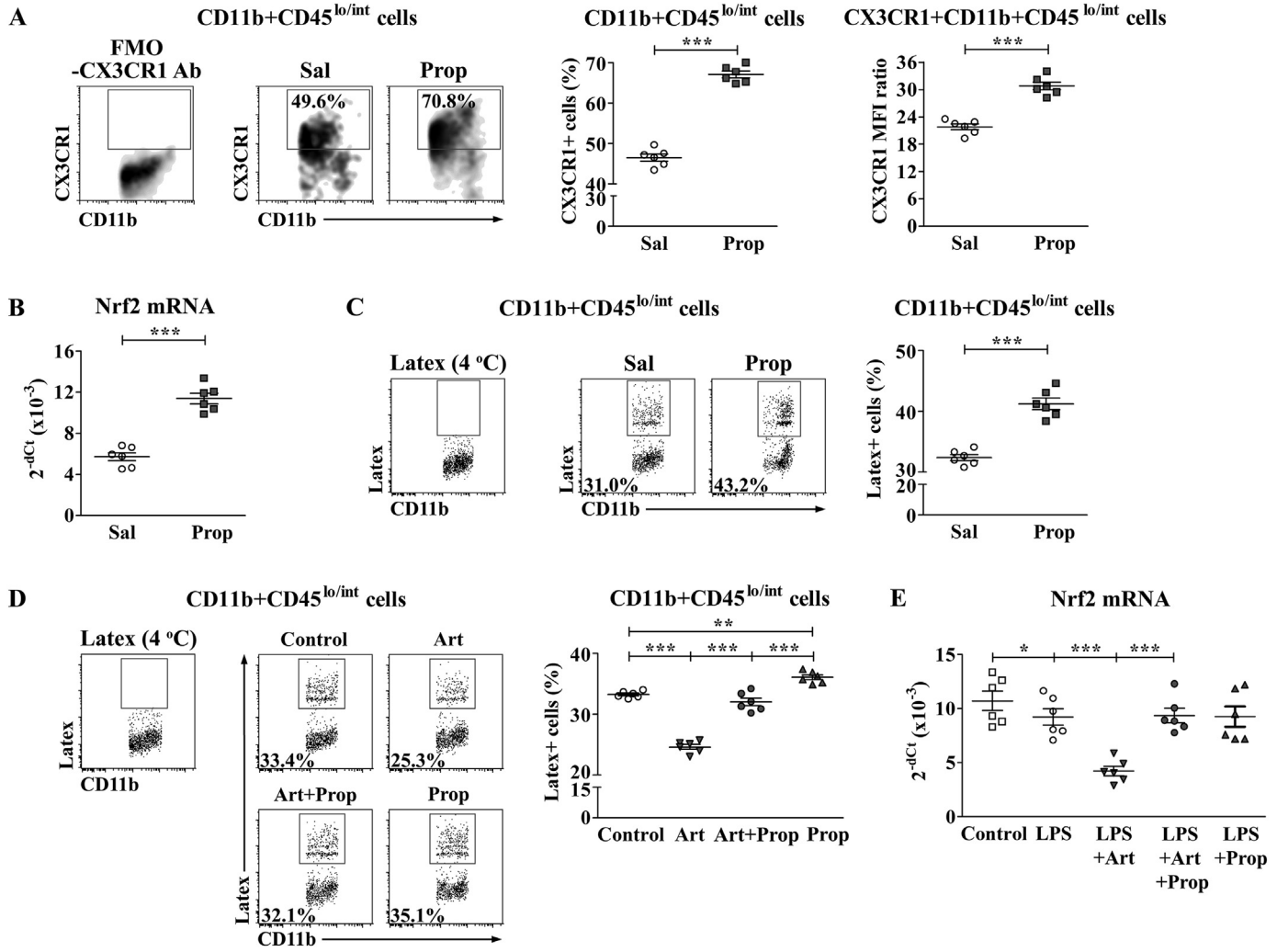

Fig. 3. Propranolol increases the frequencies of CX3CR1-expressing microglia and microglial cells exhibiting neuroprotective/immunoregulatory properties. (A) Right flow cytometry density plot panel indicates the frequency of CX3CR1+ cells among spinal cord CD11b+CD45$^{lo/int}$ microglia retrieved from rats immunized for EAE (EAE rats) on the 14th d.p.i., after (right) propranolol (Prop) or (left) saline (Sal) administration starting from the 8th d.p.i. Gating strategy for CD11b+CD45$^{lo/int}$ cells is shown in Fig. 1B. FMO control incubated with secondary antibody (Ab) alone, without anti-CX3CR1 Ab (-CX3CR1 Ab), was used to settle the gating boundary for CX3CR1+ cells. Scatter plots indicate (left) the frequency of CX3CR1+ cells among CD11b+CD45$^{lo/int}$ microglia, and (right) CX3CR1 MFI on the CX3CR1+CD11b+CD45$^{lo/int}$ cells from Prop and Sal EAE rats. **(B)** Scatter plot indicates relative expression level of nuclear factor (erythroid-derived 2)-like 2 (Nrf2) mRNA in spinal cord mononuclear cells from Prop and Sal EAE rats, determined by RT-qPCR and shown as 2^{-dCt} values relative to β-actin. **(C)** Right flow cytometry dot plot panel indicates the frequency of fluorescent latex bead-containing (Latex+) cells among spinal cord CD11b+CD45$^{lo/int}$ microglia retrieved from Prop and Sal EAE rats. Scatter plot indicates the frequency of Latex+ cells among CD11b+CD45$^{lo/int}$ microglia from Prop and Sal EAE rats. **(D)** Right flow cytometry dot plot panel indicates the frequency of Latex+ cells among CD11b+CD45$^{lo/int}$ microglia in cultures of spinal cord cells retrieved from EAE rats on the 14th d.p.i. and grown in the absence (Control) or in the presence of 10^{-6} M of arterenol (Art) and/or 10^{-5} M of Prop (see Materials and methods). Scatter plot indicates the frequency of Latex+ cells among CD11b+CD45$^{lo/int}$ microglia in spinal cord cell cultures supplemented with Art and/or Prop and the corresponding Control cultures. **(C, D)** Left flow cytometry dot plots indicate controls incubated at 4 °C, used to settle the gating boundaries for Latex+ cells. **(E)** Scatter plot indicates Nrf2 mRNA expression in spinal cord mononuclear cells retrieved from EAE rats on the 14th d.p.i. and cultured overnight in the medium alone (Control) or stimulated with lipopolysaccharide (LPS) in the absence or in the presence of Art and/or Prop (see Materials and methods). Relative mRNA expression levels were determined by RT-qPCR and shown as 2^{-dCt} values relative to β-actin. The data are shown as mean ± SEM (n = 6 rats/group). Horizontal bars in scatter plots indicate mean values. * $p \leq .05$; ** $p \leq .01$; *** $p \leq .001$.

microglia from Prop rats compared with Sal controls (Fig. 4B).

Given that vesicles derived from apoptotic cells trigger strong CD83 upregulation on microglia (Fehr et al., 2013), CD83 surface expression on microglial cells was also investigated. The frequency of CD83+ cells was higher ($p < .001$) within CD11b+CD45$^{lo/int}$ microglia from Prop rats (Fig. 4C). Additionally, CD83 surface density was increased ($p < .01$) on CD83+ cells from Prop rats compared with Sal controls (Fig. 4C).

3.2.3. Propranolol promotes development of microglia with anti-inflammatory properties

Considering that Nrf2 exerts anti-inflammatory effects by triggering HO-1 expression. (Cuadrado and Rojo, 2008; Lastres-Becker et al., 2014), its expression in spinal cord cells was also determined. In Prop rats, the expression of HO-1 mRNA ($p < .001$) was enhanced (Fig. 5A).

Activation of CX3CR1/Nrf2/HO-1 pathway is associated not only with upregulation of anti-inflammatory cytokines, but also with prevention of transcriptional upregulation of proinflammatory cytokines, and thereby with skewing of microglia towards pro-resolution M2 phenotype (Limatola and Ransohoff, 2014; Dinkova-Kostova et al.,

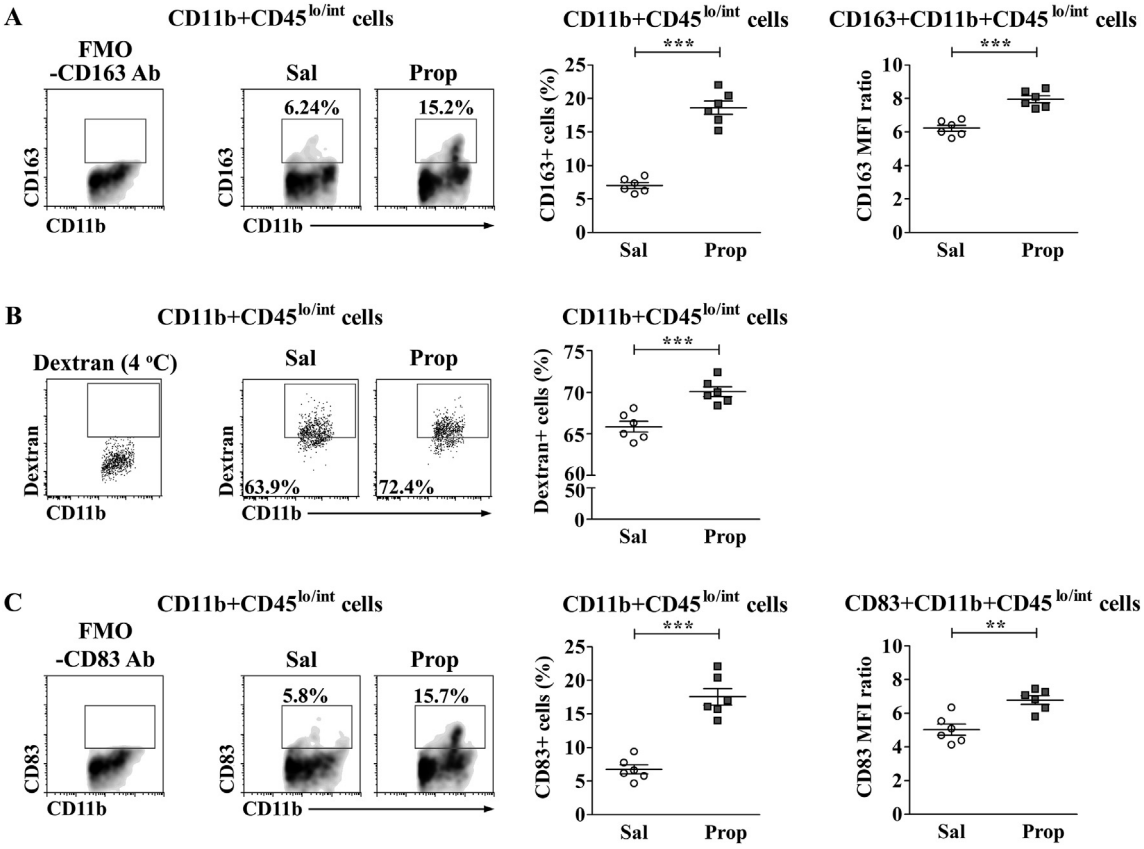

Fig. 4. Propranolol increases CD163 and CD83 expression on microglia and mannose receptor-dependent endocytosis. (A) Right flow cytometry density plot panel indicates the frequency of CD163+ cells among spinal cord CD11b+CD45$^{lo/int}$ microglia retrieved from rats immunized for EAE (EAE rats) on the 14th d.p.i., after (right) propranolol (Prop) or (left) saline (Sal) administration starting from the 8th d.p.i. Gating strategy for CD11b+CD45$^{lo/int}$ cells is shown in Fig. 1B. Scatter plots indicate (left) the frequency of CD163+ cells among CD11b+CD45$^{lo/int}$ microglia, and (right) CD163 MFI on the CD163+CD11b+CD45$^{lo/int}$ cells from Prop and Sal EAE rats. **(B)** Right flow cytometry dot plot panel indicates the frequency of dextran-containing (Dextran+) cells among spinal cord CD11b+CD45$^{lo/int}$ microglia retrieved from (right) Prop and (left) Sal EAE rats. Left flow cytometry dot plot indicates control incubated at 4 °C, used to settle the gating boundaries for Dextran+ cells. Scatter plot indicates the frequency of Dextran+ cells among CD11b+CD45$^{lo/int}$ microglia from Prop and Sal EAE rats. **(C)** Right flow cytometry density plot panel indicates the frequency of CD83+ cells among spinal cord CD11b+CD45$^{lo/int}$ microglia retrieved from (right) Prop and (left) Sal EAE rats. Scatter plots indicate (left) the frequency of CD83+ cells among CD11b+CD45$^{lo/int}$ microglia, and (right) CD83 MFI on CD83+CD11b+CD45$^{lo/int}$ cells from Prop and Sal EAE rats. **(A, C)** FMO controls incubated with **(A)** isotype control antibody (Ab) instead of anti-CD163 Ab (-CD163 Ab), or **(C)** secondary Ab alone, without anti-CD83 Ab (-CD83 Ab), were used to settle the gating boundaries for CD163+ and CD83+ cells, respectively. The data are shown as mean ± SEM (n = 6 rats/group). Horizontal bars in scatter plots indicate mean values. ** p ≤ .01; *** p ≤ .001.

2018). Accordingly, microglia was assayed for cytokine profile. Considering the crucial role of IL-10 produced by M2 microglia in the restriction of inflammation, restoration of homeostasis and promotion of tissue reparation (Lobo-Silva et al., 2016), microglia was examined for IL-10 production. In keeping with the expression of CX3CR1, Nrf2 and HO-1, the frequency of IL-10-producing cells was higher ($p < .001$) among CD11b+CD45$^{lo/int}$ microglia from Prop rats compared with Sal ones (Fig. 5B).

Microglial synthesis of IL-1β and IL-23 was also explored. The frequency of cells producing IL-1β, the cytokine whose downregulation is central for CX3CR1-mediated microglial neuroprotection (Bhaskar et al., 2010), was lower ($p < .001$) among spinal cord microglia from Prop rats compared with Sal rats (Fig. 5C). Besides, propranolol reduced ($p < .001$) the frequency of IL-23-producing cells among spinal cord microglia (Fig. 5D).

Overall, our findings indicated that propranolol could promote microglial immunomodulatory/neuroprotective functions, at least partly, independently of CX3CL1 signaling. Hence, the production of IL-10 and IL-1β in LPS-stimulated spinal cord mononuclear cells supplemented with propranolol/arterenol was also examined. Compared with control cultures, the concentration of both cytokines was increased ($p < .001$) in LPS-stimulated cultures (Fig. 5E). The addition of arterenol to these cultures decreased ($p < .001$) and increased ($p < .001$) the concentrations of IL-10 and IL-1β, respectively (Fig. 5E). The effects of arterenol were completely abrogated in the presence of propranolol (Fig. 5E). Propranolol alone increased ($p < .001$) the concentration of IL-10, but decreased ($p < .001$) that of IL-1β (Fig. 5E), thereby further supporting the synthesis of noradrenaline in microglia.

Furthermore, immunomodulatory/neuroprotective role of CX3CR1-expressing microglia may also be accomplished indirectly, through modulation of activity of astrocytes (Limatola and Ransohoff, 2014). As astrocytes are the major source of IL-6 in the CNS during inflammation (Gruol and Nelson, 1997), IL-6 mRNA in spinal cord tissue was also explored. Propranolol administration decreased ($p < .01$) the expression of IL-6 transcript in spinal cord tissue (Fig. 5F).

Finally, spinal cord mononuclear cells were investigated for the expression of mRNA for iNOS, a bona fide marker of the classically activated proinflammatory M1 microglia (Mammana et al., 2018) and mRNA for Arg-1, a typical marker of anti-inflammatory M2 microglia (Shin et al., 2012; Thompson and Tsirka, 2017). Additionally, iNOS mRNA/Arg-1 mRNA expression ratio, as an indicator of regeneration in spinal cord injury (Kigerl et al., 2009), was calculated. The expression of iNOS mRNA was downregulated ($p < .01$) (Fig. 6A), whereas that of

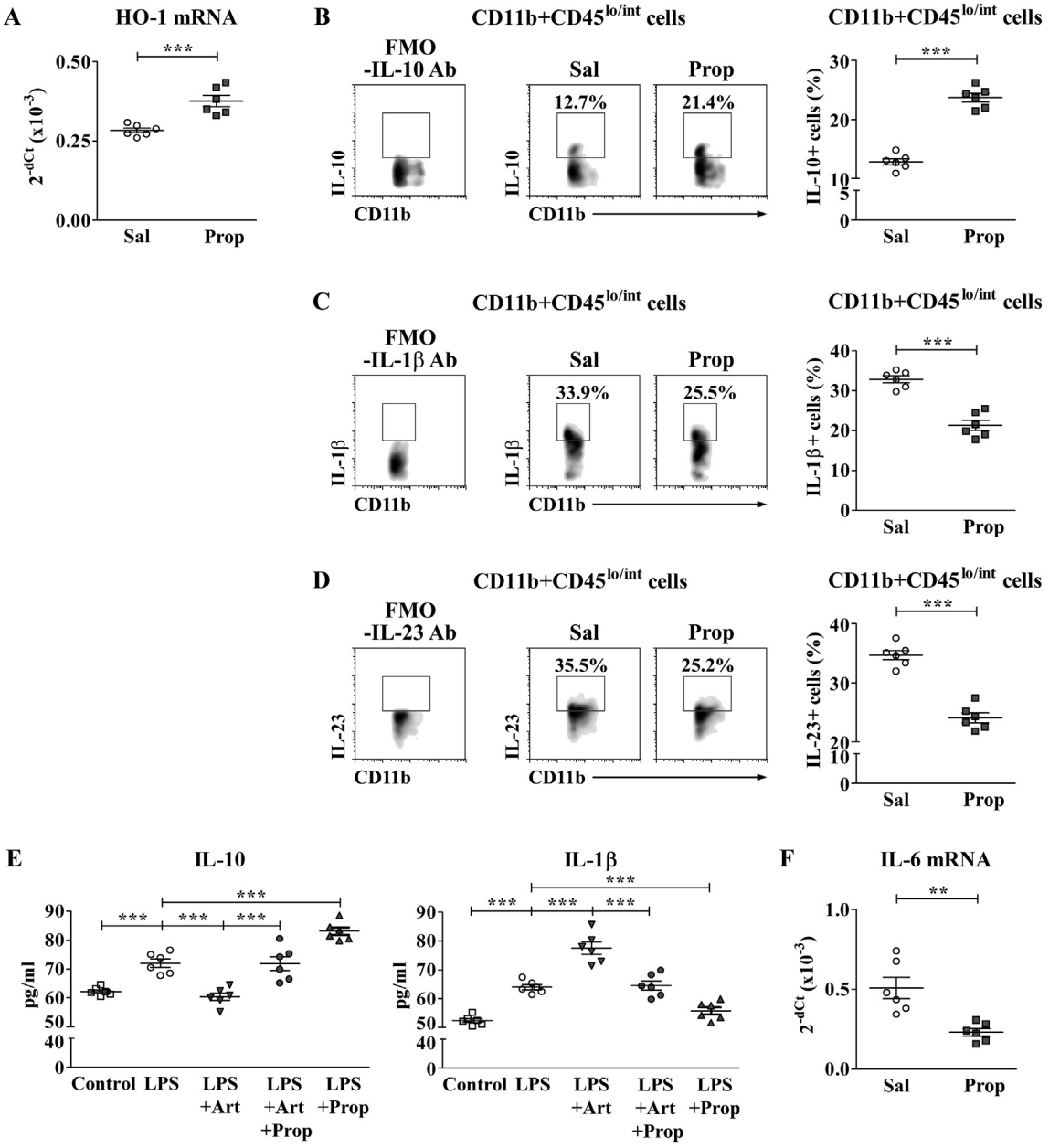

Fig. 5. Propranolol promotes anti-inflammatory functions of microglia. (A) Scatter plot indicates heme oxygenase-1 (HO-1) mRNA expression in spinal cord mononuclear cells retrieved from rats immunized for EAE (EAE rats) on the 14th d.p.i., after propranolol (Prop) or saline (Sal) administration starting from the 8th d.p.i. Relative mRNA expression levels were determined by RT-qPCR and shown as 2^{-dCt} values relative to β-actin. **(B, C, D)** Right flow cytometry density plot panels indicate the frequencies of **(B)** IL-10+, **(C)** IL-1β+ and **(D)** IL-23+ cells among spinal cord CD11b+CD45$^{lo/int}$ microglia retrieved from (right) Prop and (left) Sal EAE rats. Gating strategy for CD11b+CD45$^{lo/int}$ cells is shown in Fig. 1B. FMO controls, incubated with **(B)** isotype control antibody (Ab) instead of IL-10 Ab (-IL-10 Ab), or **(C, D)** secondary Ab alone, without IL-1β (-IL-1β Ab) or IL-23 (-IL-23 Ab) Abs, were used to settle the gating boundaries for IL-10+, IL-1β+ and IL-23+ cells, respectively. Scatter plots indicate the frequencies of **(B)** IL-10+, **(C)** IL-1β+ and **(D)** IL-23+ cells among CD11b+CD45$^{lo/int}$ microglia from Prop and Sal EAE rats. **(E)** Scatter plots indicate the concentrations of (left) IL-10 and (right) IL-1β, as determined by ELISA, in supernatants from cultures of spinal cord cells retrieved from EAE rats on the 14th d.p.i. and grown overnight in the medium alone (Control) or stimulated with LPS in the absence or in the presence of 10^{-6} M of arterenol (Art) and/or 10^{-5} M of Prop (see Materials and methods). **(F)** Scatter plot indicates relative IL-6 mRNA expression level in spinal cord tissue of Prop and Sal EAE rats, determined by RT-qPCR and shown as 2^{-dCt} value relative to β-actin. The data are shown as mean ± SEM (n = 6 rats/group). Horizontal bars in scatter plots indicate mean values. ** p ≤ .01; *** p ≤ .001.

Arg-1 mRNA was upregulated ($p < .05$) in spinal cord mononuclear cells from Prop rats compared with Sal controls (Fig. 6B). Hence, iNOS mRNA/Arg-1 mRNA expression ratio was shifted ($p < .001$) towards Arg-1 in spinal cord mononuclear cells of Prop rats (Fig. 6C).

3.2.4. Propranolol decreases the expression of MCP-1/CCL2 in spinal cord mononuclear cells

Activation of Nrf2 is shown to prevent transcriptional upregulation of chemokines, including MCP-1/CCL2 (Dinkova-Kostova et al., 2018). As MCP-1/CCL2 expressed by microglia (Semple et al., 2010) is involved in the spinal cord infiltration with blood-derived inflammatory monocytes and Th17 cells (Jiang et al., 2016), its expression in spinal cord mononuclear cells was also explored. Propranolol administration downregulated ($p < .01$) the expression of MCP-1/CCL2 mRNA (Fig. 7A). Consistently, the frequency of blood-borne myeloid cells identified as CD11b + CD45^{hi} cells (Almolda et al., 2009), was lower

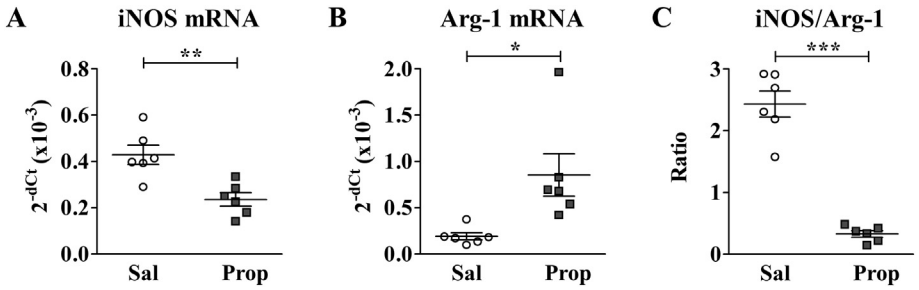

Fig. 6. Propranolol decreases iNOS/Arg-1 mRNA expression ratio in spinal cord mononuclear cells. (A, B) Scatter plots indicate **(A)** inducible nitric oxide synthase (iNOS) and **(B)** arginase (Arg-1) mRNA expression in spinal cord mononuclear cells retrieved from rats immunized for EAE (EAE rats) on the 14th d.p.i., after propranolol (Prop) or saline (Sal) administration starting from the 8th d.p.i. Relative mRNA expression levels were determined by RT-qPCR and shown as 2^{-dCt} values relative to β-actin. **(C)** Scatter plot indicates iNOS/Arg-1 mRNA expression ratio in spinal cord mononuclear cells of Prop and Sal EAE rats. The data are shown as mean ± SEM (n = 6 rats/group). Horizontal bars in scatter plots indicate mean values. * p ≤ .05; ** p ≤ .01; *** p ≤ .001.

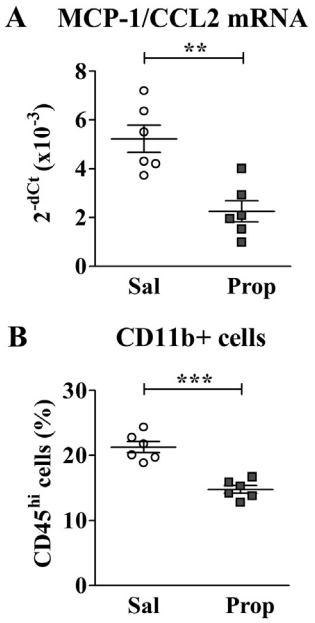

Fig. 7. Propranolol decreases the MCP-1/CCL2 mRNA expression in spinal cord mononuclear cells. (A) Scatter plot indicates MCP-1/CCL2 mRNA expression in spinal cord mononuclear cells retrieved from rats immunized for EAE (EAE rats) on the 14th d.p.i., after propranolol (Prop) or saline (Sal) administration starting from the 8th d.p.i. Relative mRNA expression levels were determined by RT-qPCR and shown as 2^{-dCt} value relative to β-actin. **(B)** Scatter plot indicates the frequency of CD11b+CD45^{hi} cells among CD11b+ spinal cord cells of Prop and Sal EAE rats. Gating strategy for CD11b+CD45^{hi} cells is shown in Fig. 1B. The data are shown as mean ± SEM (n = 6 rats/group). Horizontal bars in scatter plots indicate mean values. ** p ≤ .01; *** p ≤ .001.

(p < .001) among CD11b+ cells from Prop rats compared with Sal controls (Fig. 7B).

3.2.5. Propranolol decreases reactivation/proliferation of spinal cord-infiltrating CD4+ T cells and their differentiation into highly pathogenic Th17 cells at the peak of EAE

We found lower (p < .01) frequency of CD4+ T cells among mononuclear cells retrieved from spinal cord of Prop rats compared with Sal controls (Fig. 8A). Additionally, fewer (p < .001) spinal cord CD4+ T cells were isolated from Prop than Sal rats (Fig. 8A). Next, CD4+ T cells infiltrating EAE rat spinal cord were analyzed for the expression of activation/proliferation markers and the proinflammatory cytokines. The frequency of cells expressing CD25 activation marker was lower ($p < .05$) among CD4+Foxp3- lymphocytes retrieved from Prop rats compared with Sal ones (Fig. 8B), suggesting their impaired activation. Additionally, the frequency of cells expressing Ki-67 activation/proliferation marker among CD4+Foxp3- lymphocytes from Prop rat spinal cord was also reduced (p < .001) compared with Sal controls (Fig. 8C).

On the other hand, the frequency of Annexin V+ apoptotic cells among spinal cord-infiltrating CD4+ T lymphocytes was comparable between Prop rats and Sal controls (Fig. 8D).

Considering altered expression of the key cytokines driving/maintaining Th17 cell differentiation (IL-1β, IL-6, IL-23) (Stritesky et al., 2008; Ghoreschi et al., 2010) in Prop rats, the frequency and number of spinal cord Th17 cells were also determined. Their frequency and number were lower (p < .01) in spinal cord of Prop rats when compared with Sal ones (Fig. 9A). The synthesis of IL-17 on a per cell basis was also reduced (p < .001) in Th17 cells of Prop compared with Sal rats, judging by the IL-17 MFI (Fig. 9A). The antigen specificity of spinal cord Th17 cells was addressed in MBP recall test. In the absence of MBP (Control cultures), the frequency of IL-17–producing cells among CD4+ T cells was lower (p < .001) in spinal cord mononuclear cell cultures from Prop than in those from Sal rats (Fig. 9B). In MBP-challenged (MBP) spinal cord mononuclear cell cultures from both groups of rats, it was increased (p < .01) when compared with the corresponding Control cultures (Fig. 9B). However, the magnitude of this increase was lower (p < .001) in spinal cord cell cultures from Prop compared with Sal rats (Fig. 9B). Consequently, the frequency of Th17 cells within CD4+ T cells remained lower (p < .001) in MBP cultures from Prop rats when compared with those from Sal rats (Fig. 9B).

Considering the plasticity of Th17 cells (Cosmi et al., 2014; Kurschus, 2015), these cells were further examined for the frequency of highly pathogenic IFN-γ- and GM-CSF-producing cells (Kurschus, 2015). Propranolol reduced the frequency (p < .05) and the number (p < .01) of highly pathogenic IFN-γ+GM-CSF+ Th17 cells (Fig. 9C).

4. Discussion

The study showed changes in the spinal cord noradrenaline level and the expression of β_2-adrenoceptor on microglia during EAE course, and pointed out the mechanisms underlying noradrenaline contribution to the disease development.

4.1. Influence of immunization for EAE on the spinal cord noradrenaline level and expression of β_2-adrenoceptor on microglia

This study confirmed the previous findings indicating that noradrenaline concentration in spinal cord declines during EAE course (White et al., 1983; Krenger et al., 1986; Polak et al., 2011). AD in MS is connected with advanced stages of disease (Vlcek et al., 2018). It is suggested to contribute to disease progression and occurrence of relapses (Racosta and Kimpinski, 2016). The reduction in spinal cord noradrenaline level in EAE was ascribed to local, spinal cord, noradrenergic fiber damage (White et al., 1983). Additionally, as noradrenergic fibers terminating in rat spinal cord originate in locus coeruleus (Westlund et al., 1983), this reduction may reflect locus coeruleus

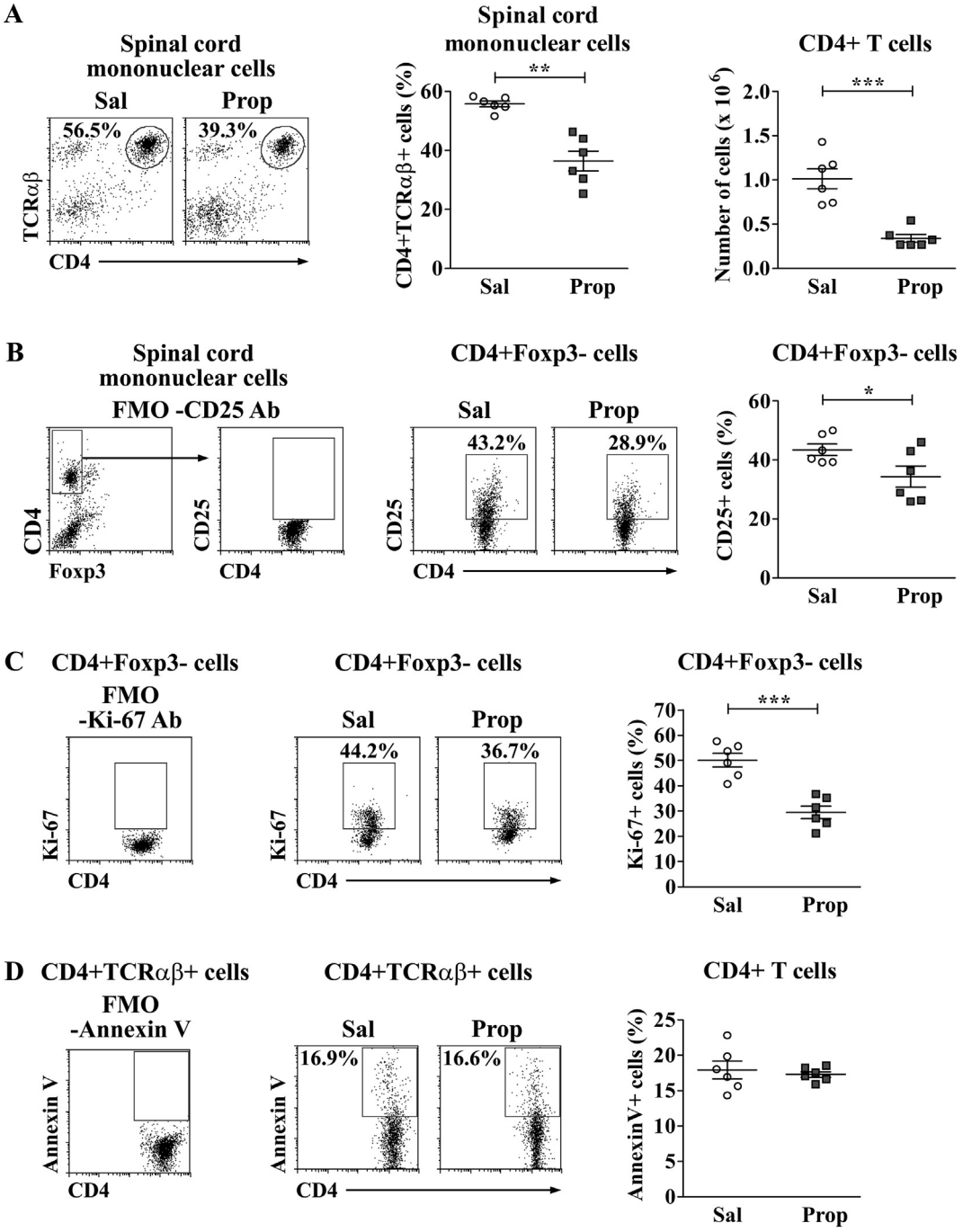

Fig. 8. Propranolol decreases the number of spinal cord-infiltrating CD4+ T cells, and the frequency of activated/proliferating cells among them. (A) Flow cytometry dot plot panel indicates the frequency of CD4+ TCRαβ+ (T) cells in spinal cords retrieved from rats immunized for EAE (EAE rats) on the 14th d.p.i., after (right) propranolol (Prop) or (left) saline (Sal) administration starting from the 8th d.p.i. Scatter plots indicate (left) the frequency and (right) the number of CD4+ T cells in spinal cords of Prop and Sal EAE rats. **(B, C)** Right flow cytometry dot plot panels indicate the frequencies of **(B)** CD25+ and **(C)** Ki-67+ cells among spinal cord CD4+Foxp3- cells retrieved from (right) Prop and (left) Sal EAE rats. FMO controls incubated with isotype control antibodies (Abs) instead of **(B)** anti-CD25 (-CD25 Ab) or **(C)** anti-Ki-67 (-Ki-67 Ab) Abs were used to settle the gating boundaries for CD25+ and Ki-67+ cells among CD4+Foxp3- lymphocytes, gated as shown in (B, utmost left). Scatter plots indicate the frequencies of **(B)** CD25+ and **(C)** Ki-67+ cells among CD4+Foxp3- lymphocytes from Prop and Sal EAE rats. **(D)** Right flow cytometry dot plot panel indicates the frequency of Annexin V+ cells among spinal cord CD4+ T cells retrieved from (right) Prop and (left) Sal EAE rats. CD4+ T cells were gated as shown in (A). FMO control without Annexin V (-Annexin V) was used to settle the gating boundary for Annexin V+ cells. Scatter plot indicates the frequency of Annexin V+ cells among CD4+ T cells of Prop and Sal EAE rats. The data are shown as mean ± SEM (n = 6 rats/group). Horizontal bars in scatter plots indicate mean values. * $p \leq .05$; ** $p \leq .01$; *** $p \leq .001$.

damage (Polak et al., 2011). Indeed, the central (locus coeruleus) noradrenaline depletion modulates clinical course of chronic relapsing rat EAE, so that each new attack is milder than the preceding ones (Krenger et al., 1986). Adding to the complexity, our findings showed the increase in expression of tyrosine hydroxylase in microglia with EAE development. This is consistent with data indicating that stimulation of myeloid cells with LPS or bacteria activates intrinsic synthesis of catecholamines to provide a self-amplifying feed-forward loop (Staedtke et al., 2018). This loop contributes to dysregulation of proinflammatory cytokine secretion leading to augmentation of

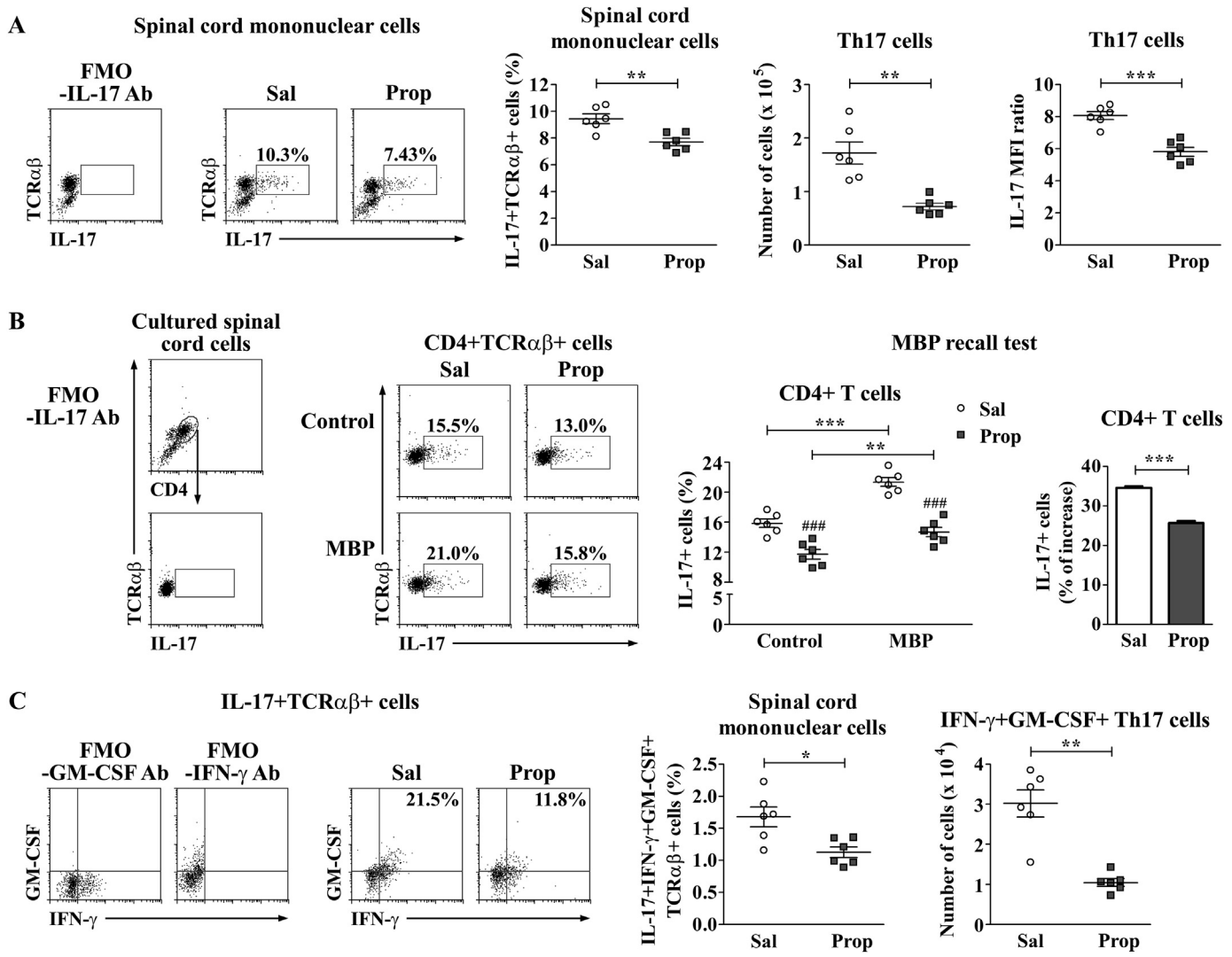

Fig. 9. Propranolol decreases the number of spinal cord-infiltrating IL-17 + TCRαβ + cells, including the highly pathogenic IFN-γ/GM-CSF co-producing ones. (A) Right flow cytometry dot plot panel indicates the frequency IL-17 + TCRαβ + (Th17) cells within spinal cord mononuclear cells retrieved from rats immunized for EAE (EAE rats) on the 14th d.p.i., after (right) propranolol (Prop) or (left) saline (Sal) administration starting from the 8th d.p.i. FMO control incubated with isotype control antibody (Ab) instead of anti-IL-17 Ab (-IL-17 Ab) was used to settle the gating boundary for IL-17 + cells. Scatter plots indicate (left) the frequency and (middle) the number of Th17 cells in spinal cords, and (right) IL-17 MFI in Th17 cells of Prop and Sal EAE rats. **(B)** Right flow cytometry dot plot panel indicates the frequency of IL-17 + cells among CD4 + TCRαβ + (T) lymphocytes in cultures of spinal cord cells retrieved from (right) Prop and (left) Sal EAE rats and grown overnight (lower) in the presence of MBP (MBP) or (upper) in its absence (Control) (see Materials and methods). FMO control incubated with isotype control Ab instead of anti-IL-17 Ab (-IL-17 Ab) was used to (lower) settle the gating boundary for IL-17 + cells among (upper) gated CD4 + T cells. Scatter plot indicates the frequency of IL-17 + cells among CD4 + T cells from MBP and corresponding Control spinal cord cell cultures from Prop and Sal EAE rats. Bar graph indicates the percentage of increase in the frequency of IL-17 + cells among spinal cord CD4 + T cells from MBP cultures over the corresponding Control cultures from Prop and Sal EAE rats. Two-way ANOVA (treatment × culturing conditions) showed significant interaction between the factors for the frequency of IL-17 + cells among CD4 + T cells ($F_{(1,20)} = 4.38$; $p < .05$). Bonferroni *post-hoc* test was used. **(C)** Right flow cytometry dot plot panel indicates the frequency of IFN-γ + GM-CSF + cells among spinal cord Th17 cells retrieved from (right) Prop and (left) Sal EAE rats. Th17 cells were gated as shown in (A). FMO controls incubated with isotype control Abs instead of (left) anti-GM-CSF (-GM-CSF Ab) and (right) anti-IFN-γ (-IFN-γ Ab) Abs were used to settle the gating boundaries for IFN-γ + GM-CSF + cells. Scatter plots indicate (left) the frequency and (right) the number of IFN-γ + GM-CSF + Th17 cells in spinal cords of Prop and Sal EAE rats. The frequency of spinal cord IFN-γ + GM-CSF + Th17 cells was determined using FlowJo software version 7.8. (TreeStar Inc., Ashland, OR, USA). The data are shown as mean ± SEM (n = 6 rats/group). Horizontal bars in scatter plots indicate mean values. * p ≤ .05; ** p ≤ .01; *** p ≤ .001; ### p ≤ .001. # vs Sal.

inflammation and tissue injury (Staedtke et al., 2018; Flierl et al., 2007). It was also suggested that some other catecholamine-producing cells participate in this feed-forward loop (Staedtke et al., 2018). Consistently, we found augmented expression of tyrosine hydroxylase in CD4 + T cells recovered from EAE rat spinal cord compared with non-immunized animals (Supplementary Fig. 1). Similarly, the frequency of noradrenaline-synthesizing ("noradrenergic") cells in the target tissues increases with the development of collagen-induced arthritis (Capellino et al., 2012). This is suggested to be a mechanism contributing to compensation for the loss of sympathetic nerve fibers (Capellino et al., 2012). Central 6-hydroxydopamine-induced depletion of catecholamines before the immunization for EAE prevented the disease development (Abramsky et al., 1987; Konkol et al., 1990). Thus, it may be assumed that they have an important role in EAE pathogenesis. Consistently, propranolol administration initiated before the appearance of the clinical signs of EAE diminished the severity of neurological deficit and duration of the disease. However, in some other studies propranolol treatment over the effector phase of rat EAE either worsened the disease (Brosnan et al., 1985) or did not affect its severity (Chelmicka-Schorr et al., 1989). These inconsistencies may be related to

differences in EAE models in respect of immunization protocol, rat strain, propranolol dosage and/or duration of the drug administration (Chelmicka-Schorr et al., 1989).

4.2. Propranolol administration over the effector phase of EAE moderates the disease course by increasing immunomodulatory/protective capacity of microglia

Our further research was focused on microglia. To justify this approach, in accordance with some other studies (Tanaka et al., 2002; Hertz et al., 2010), β_2-adrenoceptor was detected on the surface of microglia. Additionally, β_2-adrenoceptor expression on microglia increased with EAE development. This was consistent with data indicating that local decrease in noradrenaline concentration leads to upregulation of β_2-adrenoceptor expression on immune cells (Lorton and Bellinger, 2015). Several other facts strengthened our interest in microglia. Firstly, various stress paradigms induce microglial activation and upregulation of expression of proinflammatory cytokines and chemokines, and thereby exaggerate inflammatory response (Blandino Jr. et al., 2006). Secondly, these effects of stress involve catecholamine-dependent mechanisms (Wohleb et al., 2015). Thirdly, stress-induced proinflammatory microglial changes are preventable by propranolol administration (Wohleb et al., 2011). Additionally, stress is shown to decrease the expression of CX3CR1 (Wohleb et al., 2014), the key immunoregulatory molecule in neuron-microglial cell cross-talk (Biber et al., 2007). Consistently, propranolol administration to EAE rats increased the proportion of CX3CR1-expressing cells in microglia. CX3CR1 deficiency confers exacerbated EAE, as shown by severe inflammation and neuronal loss (Cardona et al., 2018). Thus, the increase in the frequency of CX3CR1-expressing cells among microglia from Prop rats was fully consistent with the greater expression of mRNA for Nrf2 in their mononuclear spinal cord cells (Castro-Sánchez et al., 2019). To corroborate the previous notion, rapid development and more severe clinical presentation of EAE were associated with greater microglial activation followed by downregulation of Nrf2 (Johnson et al., 2010). Furthermore, augmented phagocytic capacity of microglia from Prop rats could be related to the increased expression of Nrf2, as it was shown to upregulate TAM receptor expression (Castro-Sánchez et al., 2019). To additionally corroborate our findings, impaired phagocytic activity of microglia was found in the absence of CX3CR1 expression in cuprizone model of demyelination (Lampron et al., 2015). However, the analysis of the effects of arterenol on phagocytic capacity of microglia *in vitro* suggested that noradrenaline, acting through β-adrenoceptor, could diminish microglial phagocytosis in a CX3CR1-independent manner, as well. Indeed, catecholamines are shown to impair splenic macrophage phagocytosis *in vitro* (Roy and Rai, 2004). Additionally, as propranolol counteracted arterenol-induced downregulation of Nrf2 expression in LPS-stimulated spinal cord mononuclear cell cultures, it may be assumed that propranolol effect on phagocytosis was mediated by Nrf2. This assumption is consistent with findings obtained in several other studies. Carvedilol, a third-generation β-blocker, activated Nrf2 signaling pathway in HT22 murine hippocampal neuronal cell line (Ouyang et al., 2013) and PC12 rat pheochromocytoma cell line (Wang et al., 2014). Additionally, in the rat model of sepsis, propranolol induced the expression of the gene encoding HO-1 (Wilson et al., 2013), often used as a marker of Nrf2-dependent anti-inflammatory response (Lastres-Becker et al., 2014).

In accordance with the increase in phagocytic capacity of microglia (A-Gonzalez et al., 2017), the expression of CD163 was upregulated on microglia from Prop rats. To add extra weight to this finding are data indicating that the increased frequency of CD163+ microglial cells is associated with down-modulation of neuroinflammation in acute model of EAE, and consequent recovery from paralysis (Ahn et al., 2012). In accordance with enhanced phagocytic capacity of microglia, the mannose-receptor–mediated endocytosis by microglia from Prop rats was enhanced. Namely, phagocyting cells are shown to upregulate not only CD163 expression, but also that of Mrc1 gene (encoding for CD206, the mannose receptor) (A-Gonzalez et al., 2017; Mammana et al., 2018). Moreover, the enhanced phagocytosis by microglial cells from Prop rats correlated with upregulation in CD83 expression (Fehr et al., 2013). The latter could be associated with acquisition of regulatory/regenerative phenotype by microglia (Olah et al., 2012) and down-modulation of Th cell-initiated tissue damage (Fujimoto and Tedder, 2006; Stojić-Vukanić et al., 2018).

Next, enhanced expression of the components of CX3CR1-Nrf2 axis correlated with upregulation of HO-1-encoding gene in Prop rats (Lastres-Becker et al., 2014; Castro-Sánchez et al., 2019). Consistently, the proportion of microglia expressing anti-inflammatory IL-10 was increased in Prop rats (Dinkova-Kostova et al., 2018). It is of note that IL-10 itself is capable of inducing HO-1 production, thereby forming a positive feedback circuit to amplify the anti-inflammatory response (Lee and Chau, 2002). Propranolol-induced changes in CX3CR1-Nrf2 axis could also be linked with the decrease in the proportion of microglia expressing proinflammatory IL-1β and IL-23 cytokines (Cuadrado et al., 2014; Lastres-Becker et al., 2014; Castro-Sánchez et al., 2019). The former is particularly important as microglial cell-derived IL-1β is a key mediator of stress response in the CNS (Blandino Jr. et al., 2006; Wohleb et al., 2011; Frank et al., 2019). In this context, it is noteworthy that: i) stress-induced IL-1β elevation can be prevented by propranolol (Johnson et al., 2005), and ii) β-AR activation is shown to augment microglial IL-1β production (Tomozawa et al., 1995; Wang et al., 2010). Antagonizing action of propranolol on arterenol effects in LPS cultures further supports CX3CR1-independent action of propranolol on Nrf2 expression, as IL-10 and IL-1β are important targets of Nrf2/HO-1 pathway (Ambegaokar and Kolson, 2014). Moreover, propranolol downregulated IL-6 mRNA expression in spinal cord tissue. This could be ascribed to lower IL-6 expression not only in microglia (Tomozawa et al., 1995; Wang et al., 2010), but also in astrocytes, due to increased frequency of CX3CR1+ microglia (Limatola and Ransohoff, 2014).

In accordance with the shift towards a more anti-inflammatory microglial phenotype, iNOS/Arg-1 gene expression ratio was shifted towards Arg-1 expression in Prop rats compared with controls. This is consistent with upregulation of iNOS concomitant with downregulation of Arg-1 in microglia from Nrf2-deficient mice (Rojo et al., 2010).

In accordance with the decreased expression of MCP-1/CCL2 in spinal cord cells, fewer CD4+ T lymphocytes were recovered from spinal cord of Prop rats (Semple et al., 2010). Additionally, the shift towards more anti-inflammatory phenotypic and functional properties of microglia from Prop rats correlated with fewer activated/proliferating cells among CD4+ T lymphocytes compared with controls (Schetters et al., 2018). Specifically, CX3CR1 upregulation on microglia is associated with impaired T-cell proliferation (Krasemann et al., 2017). Additionally, suppressive effect of propranolol on T-cell reactivation/proliferation could also be partly associated with the increased microglial IL-10 production and CD83 expression (Lobo-Silva et al., 2016; Stojić-Vukanić et al., 2018). A less efficient activation of CD4+ T cells is shown to render them more susceptible to apoptosis (Rogers et al., 2001). The lack of differences in the frequency of apoptotic cells among spinal cord CD4+ T cells from Prop and control rats could be linked with the increased microglial phagocytic capacity, and consequently more efficient removal of apoptotic cells in Prop rats.

In accordance with the decrease in IL-1β, IL-6 and IL-23 production/expression, the frequency of spinal cord Th17 cells, and the most pathogenic IFN-γ+GM-CSF+ Th17 ones, was reduced in Prop rats compared with controls (Mufazalov et al., 2017). Thus, this could also contribute to neurologically milder disease.

In conclusion, this study provided novel data contributing to our understanding of the role of β-adrenoceptor–mediated action of central noradrenaline in the development of clinical EAE. It indicates that noradrenaline, through β-adrenoceptor, may modulate microglial functional properties via both CX3CR1-dependent and possibly

CX3CR1-independent mechanisms, and consequently severity of neurological deficit in EAE. The putative clinical implications of these findings are two-fold. Firstly, they suggest that microglial CX3CR1-Nrf2/TAM(HO-1) signaling pathways should be considered as a possible therapeutic target not only in neurodegenerative diseases (Jazwa and Cuadrado, 2010), but also in MS. In this respect, propranolol, as a drug with safe pharmacological profile, could be a putative therapeutic option. Secondly, the differences between herein described central and previously reported peripheral effects of propranolol on immune cells (Vujnović et al., 2019) suggest that caution is needed when the use of blood-brain barrier–penetrating β-adrenoceptor targeting drugs in therapy of MS is considered.

Supplementary data to this article can be found online at https://doi.org/10.1016/j.nbd.2019.104665.

Funding

This work was supported by the Ministry of Education, Science and Technological Development of the Republic of Serbia [grant number 175050].

The funding source has not been involved in any way in the study design, collection, analysis and interpretation of data, writing of the manuscript and the decision to submit the manuscript for publication.

Declaration of competing interest

None.

References

Abramsky, O., Wertman, E., Reches, A., Brenner, T., Ovadia, H., 1987. Effect of hypothalamic lesions on experimental autoimmune diseases in rats. Ann. N. Y. Acad. Sci. 496, 360–365. https://doi.org/10.1111/j.1749-6632.1987.tb35788.x.

A-Gonzalez, N., Quintana, J.A., García-Silva, S., Mazariegos, M., González de la Aleja, A., Nicolás-Ávila, J.A., Walter, W., Adrover, J.M., Crainiciuc, G., Kuchroo, V.K., Rothlin, C.V., Peinado, H., Castrillo, A., Ricote, M., Hidalgo, A., 2017. Phagocytosis imprints heterogeneity in tissue-resident macrophages. J. Exp. Med. 214, 1281–1296. https://doi.org/10.1084/jem.20161375.

Ahn, M., Yang, W., Kim, H., Jin, J.K., Moon, C., Shin, T., 2012. Immunohistochemical study of arginase-1 in the spinal cords of Lewis rats with experimental autoimmune encephalomyelitis. Brain Res. 1453, 77–86. https://doi.org/10.1016/j.brainres.2012.03.023.

Almolda, B., Costa, M., Montoya, M., González, B., Castellano, B., 2009. CD4 microglial expression correlates with spontaneous clinical improvement in the acute Lewis rat EAE model. J. Neuroimmunol. 209, 65–80. https://doi.org/10.1016/j.jneuroim.2009.01.026.

Alvarez, D.F., Helm, K., DeGregori, J., Roederer, M., Majka, S., 2010. Publishing flow cytometry data. Am. J. Physiol. Lung. Cell. Mol. Physiol. 298, L127–L130. https://doi.org/10.1152/ajplung.00313.2009.

Ambegaokar, S.S., Kolson, D.L., 2014. Heme oxygenase-1 dysregulation in the brain: implications for HIV associated neurocognitive disorders. Curr. HIV Res. 12, 174–188. https://doi.org/10.2174/1570162X12666140526122709.

Bhaskar, K., Konerth, M., Kokiko-Cochran, O.N., Cardona, A., Ransohoff, R.M., Lamb, B.T., 2010. Regulation of tau pathology by the microglial fractalkine receptor. Neuron 68, 19–31. https://doi.org/10.1016/j.neuron.2010.08.023.

Biber, K., Neumann, H., Inoue, K., Boddeke, H.W., 2007. Neuronal 'On' and 'Off' signals control microglia. Trends Neurosci. 30, 596–602. https://doi.org/10.1016/j.tins.2007.08.007.

Blandino Jr., P., Barnum, C.J., Deak, T., 2006. The involvement of norepinephrine and microglia in hypothalamic and splenic IL-1beta responses to stress. J. Neuroimmunol. 173, 87–95. https://doi.org/10.1016/j.jneuroim.2005.11.021.

Brosnan, C.F., Goldmuntz, E.A., Cammer, W., Factor, S.M., Bloom, B.R., Norton, W.T., 1985. Prazosin, an alpha 1-adrenergic receptor antagonist, suppresses experimental autoimmune encephalomyelitis in the Lewis rat. Proc. Natl. Acad. Sci. U. S. A. 82, 5915–5919. https://doi.org/10.1073/pnas.82.17.5915.

Brown, B.N., Valentin, J.E., Stewart-Akers, A.M., McCabe, G.P., Badylak, S.F., 2009. Macrophage phenotype and remodeling outcomes in response to biologic scaffolds with and without a cellular component. Biomaterials 30, 1482–1491. https://doi.org/10.1016/j.biomaterials.2008.11.040.

Capellino, S., Weber, K., Gelder, M., Härle, P., Straub, R.H., 2012. First appearance and location of catecholaminergic cells during experimental arthritis and elimination by chemical sympathectomy. Arthritis Rheum. 64, 1110–1118. https://doi.org/10.1002/art.33431.

Cardona, S.M., Kim, S.V., Church, K.A., Torres, V.O., Cleary, I.A., Mendiola, A.S., Saville, S.P., Watowich, S.S., Parker-Thornburg, J., Soto-Ospina, A., Araque, P., Ransohoff, R.M., Cardona, A.E., 2018. Role of the fractalkine receptor in CNS autoimmune inflammation: new approach utilizing a mouse model expressing the human CX3CR1$^{I249/M280}$ variant. Front. Cell. Neurosci. 12, 365. https://doi.org/10.3389/fncel.2018.00365.

Castro-Sánchez, S., García-Yagüe, Á.J., Kügler, S., Lastres-Becker, I., 2019. CX3CR1-deficient microglia shows impaired signalling of the transcription factor NRF2: implications in tauopathies. Redox Biol. 22, 101118. https://doi.org/10.1016/j.redox.2019.101118.

Chelmicka-Schorr, E., Kwasniewski, M.N., Thomas, B.E., Arnason, B.G.W., 1989. The β-adrenergic agonist isoproterenol suppresses experimental allergic encephalomyelitis in Lewis rats. J. Neuroimmunol. 25, 203–207. https://doi.org/10.1016/0165-5728(89)90138-0.

Cosmi, L., Liotta, F., Maggi, E., Romagnani, S., Annunziato, F., 2014. Th17 and non-classic Th1 cells in chronic inflammatory disorders: two sides of the same coin. Int. Arch. Allergy Immunol. 164, 171–177. https://doi.org/10.1159/000363502.

Cuadrado, A., Rojo, A.I., 2008. Heme oxygenase-1 as a therapeutic target in neurodegenerative diseases and brain infections. Curr. Pharm. Des. 14, 429–442. https://doi.org/10.2174/138161208783597407.

Cuadrado, A., Martin-Moldes, Z., Ye, J., Lastres-Becker, I., 2014. Transcription factors NRF2 and NF-kappaB are coordinated effectors of the Rho family, GTP-binding protein RAC1 during inflammation. J. Biol. Chem. 289, 15244–15258. https://doi.org/10.1074/jbc.M113.540633.

De Keyser, J., Zeinstra, E., Wilczak, N., 2004. Astrocytic beta 2-adrenergic receptors and multiple sclerosis. Neurobiol. Dis. 15, 331–339. https://doi.org/10.1016/j.nbd.2003.10.012.

del Rey, A., Besedovsky, H.O., Sorkin, E., Da Prada, M., Bondiolotti, G.P., 1982. Sympathetic immunoregulation: difference between high- and low-responder animals. Am. J. Phys. 242, R30–R33. https://doi.org/10.1152/ajpregu.1982.242.1.R30.

Dinkova-Kostova, A.T., Kostov, R.V., Kazantsev, A.G., 2018. The role of Nrf 2 signaling in counteracting neurodegenerative diseases. FEBS J. 285, 3576–3590. https://doi.org/10.1111/febs.14379.

Djikić, J., Nacka-Aleksić, M., Pilipović, I., Stojić-Vukanić, Z., Bufan, B., Kosec, D., Dimitrijević, M., Leposavić, G., 2014. Age-associated changes in rat immune system: lessons learned from experimental autoimmune encephalomyelitis. Exp. Gerontol. 58, 179–197. https://doi.org/10.1016/j.exger.2014.08.005.

Elenkov, I.J., Wilder, R.L., Chrousos, G.P., Vizi, E.S., 2000. The sympathetic nerve–an integrative interface between two supersystems: the brain and the immune system. Pharmacol. Rev. 52, 595–638.

Fehr, E.M., Spoerl, S., Heyder, P., Herrmann, M., Bekeredjian-Ding, I., Blank, N., Lorenz, H.M., Schiller, M., 2013. Apoptotic-cell-derived membrane vesicles induce an alternative maturation of human dendritic cells which is disturbed in SLE. J. Autoimmun. 40, 86–95. https://doi.org/10.1016/j.jaut.2012.08.003.

Flachenecker, P., Rufer, A., Bihler, I., Hippel, C., Reiners, K., Toyka, K.V., Kesselring, J., 2003. Fatigue in MS is related to sympathetic vasomotor dysfunction. Neurology 61, 851–853. https://doi.org/10.1212/01.wnl.0000080365.95436.b8.

Flatmark, T., 2000. Catecholamine biosynthesis and physiological regulation in neuroendocrine cells. Acta Physiol. Scand. 168, 1–17. https://doi.org/10.1046/j.1365-201x.2000.00596.x.

Flierl, M.A., Rittirsch, D., Nadeau, B.A., Chen, A.J., Sarma, J.V., Zetoune, F.S., McGuire, S.R., List, R.P., Day, D.E., Hoesel, L.M., Gao, H., Van Rooijen, N., Huber-Lang, M.S., Neubig, R.R., Ward, P.A., 2007. Phagocyte-derived catecholamines enhance acute inflammatory injury. Nature 449, 721–725. https://doi.org/10.1038/nature06185.

Frank, M.G., Fonken, L.K., Watkins, L.R., Maier, S.F., 2019. Microglia: neuroimmune-sensors of stress. Semin. Cell Dev. Biol. https://doi.org/10.1016/j.semcdb.2019.01.001.

Fujimoto, Y., Tedder, T.F., 2006. CD83: a regulatory molecule of the immune system with great potential for therapeutic application. J. Med. Dent. Sci. 53, 85–91.

Ghoreschi, K., Laurence, A., Yang, X.P., Tato, C.M., McGeachy, M.J., Konkel, J.E., Ramos, H.L., Wei, L., Davidson, T.S., Bouladoux, N., Grainger, J.R., Chen, Q., Kanno, Y., Watford, W.T., Sun, H.W., Eberl, G., Shevach, E.M., Belkaid, Y., Cua, D.J., Chen, W., O'Shea, J.J., 2010. Generation of pathogenic T(H)17 cells in the absence of TGF-β signalling. Nature 467, 967–971. https://doi.org/10.1038/nature09447.

Gruol, D.L., Nelson, T.E., 1997. Physiological and pathological roles of interleukin-6 in the central nervous system. Mol. Neurobiol. 15, 307–339. https://doi.org/10.1007/BF02740665.

Haensch, C.A., Jörg, J., 2006. Autonomic dysfunction in multiple sclerosis. J. Neurol. 253, I3–I9. https://doi.org/10.1007/s00415-006-1102-2.

Hertz, L., Lovatt, D., Goldman, S.A., Nedergaard, M., 2010. Adrenoceptors in brain: cellular gene expression and effects on astrocytic metabolism and [Ca(2+)]i. Neurochem. Int. 57, 411–420. https://doi.org/10.1016/j.neuint.2010.03.019.

Hill, N.J., Hultcrantz, M., Sarvetnick, N., Flodström-Tullberg, M., 2007. The target tissue in autoimmunity–an influential niche. Eur. J. Immunol. 37, 589–597. https://doi.org/10.1002/eji.200636368.

Jazwa, A., Cuadrado, A., 2010. Targeting heme oxygenase-1 for neuroprotection and neuroinflammation in neurodegenerative diseases. Curr. Drug Targets 11, 1517–1531. https://doi.org/10.2174/1389450111009011517.

Ji, R., Meng, L., Li, Q., Lu, Q., 2015. TAM receptor deficiency affects adult hippocampal neurogenesis. Metab. Brain Dis. 30, 633–644. https://doi.org/10.1007/s11011-014-9636-y.

Jiang, W., St-Pierre, S., Roy, P., Morley, B.J., Hao, J., Simard, A.R., 2016. Infiltration of CCR2+Ly6Chigh proinflammatory monocytes and neutrophils into the central nervous system is modulated by nicotinic acetylcholine receptors in a model of multiple sclerosis. J. Immunol. 196, 2095–2108. https://doi.org/10.4049/jimmunol.1501613.

Johnson, J.D., Campisi, J., Sharkey, C.M., Kennedy, S.L., Nickerson, M., Greenwood, B.N., Fleshner, M., 2005. Catecholamines mediate stress-induced increases in peripheral and central inflammatory cytokines. Neuroscience 135, 1295–1307. https://doi.org/10.1016/j.neuroscience.2005.06.090.

Johnson, D.A., Amirahmadi, S., Ward, C., Fabry, Z., Johnson, J.A., 2010. The absence of the pro-antioxidant transcription factor Nrf2 exacerbates experimental autoimmune encephalomyelitis. Toxicol. Sci. 114, 237–246. https://doi.org/10.1093/toxsci/kfp274.

Karaszewski, J.W., Reader, A.T., Maselli, R., Brown, M., Arnason, B.G., 1990. Sympathetic skin responses are decreased and lymphocyte beta-adrenoreceptors are increased in progressive multiple sclerosis. Ann. Neurol. 27, 107–117. https://doi.org/10.1002/ana.410270404.

Kawakami, N., Lassmann, S., Li, Z., Odoardi, F., Ritter, T., Ziemssen, T., Klinkert, W.E., Ellwart, J.W., Bradl, M., Krivacic, K., Lassmann, H., Ransohoff, R.M., Volk, H.D., Wekerle, H., Linington, C., Flügel, A., 2004. The activation status of neuroantigen-specific T cells in the target organ determines the clinical outcome of autoimmune encephalomyelitis. J. Exp. Med. 199, 185–197. https://doi.org/10.1084/jem.20031064.

Kigerl, K.A., Gensel, J.C., Ankeny, D.P., Alexander, J.K., Donnelly, D.J., Popovich, P.G., 2009. Identification of two distinct macrophage subsets with divergent effects causing either neurotoxicity or regeneration in the injured mouse spinal cord. J. Neurosci. 29, 13435–13444. https://doi.org/10.1523/JNEUROSCI.3257-09.2009.

Kim, H., Moon, C., Ahn, M., Lee, Y., Kim, S., Matsumoto, Y., Koh, C.S., Kim, M.D., Shin, T., 2007. Increased phosphorylation of cyclic AMP response element-binding protein in the spinal cord of Lewis rats with experimental autoimmune encephalomyelitis. Brain Res. 1162, 113–120. https://doi.org/10.1016/j.brainres.2007.05.072.

Kodounis, A., Stamboulis, E., Constantinidis, T.S., Liolios, A., 2005. Measurement of autonomic dysregulation in multiple sclerosis. Acta Neurol. Scand. 112, 403–408. https://doi.org/10.1111/j.1600-0404.2005.00446.x.

Konkol, R.J., Wesselmann, U., Karpus, W.J., Leo, G.L., Killen, J.A., Roerig, D.L., 1990. Suppression of clinical weakness in experimental autoimmune encephalomyelitis associated with weight changes, and post-decapitation convulsions after intracisternal-ventricular administration of 6-hydroxydopamine. J. Neuroimmunol. 26, 25–34. https://doi.org/10.1016/0165-5728(90)90116-5.

Krasemann, S., Madore, C., Cialic, R., Baufeld, C., Calcagno, N., El Fatimy, R., Beckers, L., O'Loughlin, E., Xu, Y., Fanek, Z., Greco, D.J., Smith, S.T., Tweet, G., Humulock, Z., Zrzavy, T., Conde-Sanroman, P., Gacias, M., Weng, Z., Chen, H., Tjon, E., Mazaheri, F., Hartmann, K., Madi, A., Ulrich, J.D., Glatzel, M., Worthmann, A., Heeren, J., Budnik, B., Lemere, C., Ikezu, T., Heppner, F.L., Litvak, V., Holtzman, D.M., Lassmann, H., Weiner, H.L., Ochando, J., Haass, C., Butovsky, O., 2017. The TREM2-APOE pathway drives the transcriptional phenotype of dysfunctional microglia in neurodegenerative diseases. Immunity 47, 566–581.e9. https://doi.org/10.1016/j.immuni.2017.08.008.

Krenger, W., Honegger, C.G., Feurer, C., Cammisuli, S., 1986. Changes of neurotransmitter systems in chronic relapsing experimental allergic encephalomyelitis in rat brain and spinal cord. J. Neurochem. 47, 1247–1254. https://doi.org/10.1111/j.1471-4159.1986.tb00747.x.

Kurschus, F.C., 2015. T cell mediated pathogenesis in EAE: molecular mechanisms. Biom. J. 38, 183–193. https://doi.org/10.4103/2319-4170.155590.

Lampron, A., Larochelle, A., Laflamme, N., Préfontaine, P., Plante, M.M., Sánchez, M.G., Yong, V.W., Stys, P.K., Tremblay, M.È., Rivest, S., 2015. Inefficient clearance of myelin debris by microglia impairs remyelinating processes. J. Exp. Med. 212, 481–495. https://doi.org/10.1084/jem.20141656.

Lassmann, H., van Horssen, J., 2011. The molecular basis of neurodegeneration in multiple sclerosis. FEBS Lett. 585, 3715–3723. https://doi.org/10.1016/j.febslet.2011.08.004.

Lastres-Becker, I., Innamorato, N.G., Jaworski, T., Rabano, A., Kugler, S., Van Leuven, F., Cuadrado, A., 2014. Fractalkine activates NRF2/NFE2L2 and heme oxygenase 1 to restrain tauopathy-induced microgliosis. Brain 137, 78–91. https://doi.org/10.1093/brain/awt323.

Laukova, M., Vargovic, P., Vlcek, M., Lejavova, K., Hudecova, S., Krizanova, O., Kvetnansky, R., 2013. Catecholamine production is differently regulated in splenic T- and B-cells following stress exposure. Immunobiology 218, 780–789. https://doi.org/10.1016/j.imbio.2012.08.279.

Lee, T.S., Chau, L.Y., 2002. Heme oxygenase-1 mediates the anti-inflammatory effect of interleukin-10 in mice. Nat. Med. 8, 240–246. https://doi.org/10.1038/nm0302-240.

Leonard, J.P., Mac Kenzie, F.J., Patel, H.A., Cuzner, M.L., 1990. Splenic noradrenergic and adrenocortical responses during the preclinical and clinical stages of adoptively transferred experimental autoimmune encephalomyelitis (EAE). J. Neuroimmunol. 26, 183–186. https://doi.org/10.1016/0165-5728(90)90090-A.

Limatola, C., Ransohoff, R.M., 2014. Modulating neurotoxicity through CX3CL1/CX3CR1 signaling. Front. Cell. Neurosci. 8, 229. https://doi.org/10.3389/fncel.2014.00229.

Lobo-Silva, D., Carriche, G.M., Castro, A.G., Roque, S., Saraiva, M., 2016. Balancing the immune response in the brain: IL-10 and its regulation. J. Neuroinflammation 13, 297. https://doi.org/10.1186/s12974-016-0763-8.

Lorton, D., Bellinger, D.L., 2015. Molecular mechanisms underlying β-adrenergic receptor-mediated cross-talk between sympathetic neurons and immune cells. Int. J. Mol. Sci. 16, 5635–5665. https://doi.org/10.3390/ijms16035635.

Mackenzie, F.J., Leonard, J.P., Cuzner, M.L., 1989. Changes in lymphocyte beta-adrenergic receptor density and noradrenaline content of the spleen are early indicators of immune reactivity in acute experimental allergic encephalomyelitis in the Lewis rat. J. Neuroimmunol. 23, 93–100. https://doi.org/10.1016/0165-5728(89)90027-1.

Mammana, S., Fagone, P., Cavalli, E., Basile, M.S., Petralia, M.C., Nicoletti, F., Bramanti, P., Mazzon, E., 2018. The role of macrophages in neuroinflammatory and neurodegenerative pathways of Alzheimer's disease, amyotrophic lateral sclerosis, and multiple sclerosis: pathogenetic cellular effectors and potential therapeutic targets. Int. J. Mol. Sci. 19, 831. https://doi.org/10.3390/ijms19030831.

Mufazalov, I.A., Schelmbauer, C., Regen, T., Kuschmann, J., Wanke, F., Gabriel, L.A., Hauptmann, J., Müller, W., Pinteaux, E., Kurschus, F.C., Waisman, A., 2017. IL-1 signaling is critical for expansion but not generation of autoreactive GM-CSF+ Th17 cells. EMBO J. 36, 102–115. https://doi.org/10.15252/embj.201694615.

Nacka-Aleksić, M., Djikić, J., Pilipović, I., Stojić-Vukanić, Z., Kosec, D., Bufan, B., Arsenović-Ranin, N., Dimitrijević, M., Leposavić, G., 2015. Male rats develop more severe experimental autoimmune encephalomyelitis than female rats: sexual dimorphism and diergism at the spinal cord level. Brain Behav. Immun. 49, 101–118. https://doi.org/10.1016/j.bbi.2015.04.017.

Nance, D.M., Sanders, V.M., 2007. Autonomic innervation and regulation of the immune system (1987-2007). Brain Behav. Immun. 21, 736–745. https://doi.org/10.1016/j.bbi.2007.03.008.

Neil-Dwyer, G., Bartlett, J., McAinsh, J., Cruickshank, J.M., 1981. Beta-adrenoceptor blockers and the blood-brain barrier. Br. J. Clin. Pharmacol. 11, 549–553. https://doi.org/10.1111/j.1365-2125.1981.tb01169.x.

Olah, M., Amor, S., Brouwer, N., Vinet, J., Eggen, B., Biber, K., Boddeke, H.W., 2012. Identification of a microglia phenotype supportive of remyelination. Glia 60, 306–321. https://doi.org/10.1002/glia.21266.

Ouyang, Y., Chen, Z., Tan, M., Liu, A., Chen, M., Liu, J., Pi, R., Fang, J., 2013. Carvedilol, a third-generation β-blocker prevents oxidative stress-induced neuronal death and activates Nrf2/ARE pathway in HT22 cells. Biochem. Biophys. Res. Commun. 441, 917–922. https://doi.org/10.1016/j.bbrc.2013.10.160.

Padro, C.J., Sanders, V.M., 2014. Neuroendocrine regulation of inflammation. Semin. Immunol. 26, 357–368. https://doi.org/10.1016/j.smim.2014.01.003.

Pilipović, I., Vujnović, I., Stojić-Vukanić, Z., Petrović, R., Kosec, D., Nacka-Aleksić, M., Jasnić, N., Leposavić, G., 2019a. Noradrenaline modulates CD4+ T cell priming in rat experimental autoimmune encephalomyelitis: a role for the α_1-adrenoceptor. Immunol. Res. https://doi.org/10.1007/s12026-019-09082-y.

Pilipović, I., Vujnović, I., Petrović, R., Stojić-Vukanić, Z., Leposavić, G., 2019b. Propranolol impairs primary immune responses in rat experimental autoimmune encephalomyelitis. Neuroimmunomodulation 26, 129–138. https://doi.org/10.1159/000500094.

Polak, P.E., Kalinin, S., Feinstein, D.L., 2011. Locus coeruleus damage and noradrenaline reductions in multiple sclerosis and experimental autoimmune encephalomyelitis. Brain 134, 665–677. https://doi.org/10.1093/brain/awq362.

Racosta, J.M., Kimpinski, K., 2016. Autonomic dysfunction, immune regulation, and multiple sclerosis. Clin. Auton. Res. 26, 23–31. https://doi.org/10.1007/s10286-015-0325-7.

Rajda, C., Bencsik, K., Vécsei, L.L., Bergquist, J., 2002. Catecholamine levels in peripheral blood lymphocytes from multiple sclerosis patients. J. Neuroimmunol. 124, 93–100. https://doi.org/10.1016/S0165-5728(02)00002-4.

Reguzzoni, M., Cosentino, M., Rasini, E., Marino, F., Ferrari, M., Bombelli, R., Congiu, T., Protasoni, M., Quacci, D., Lecchini, S., Raspanti, M., Frigo, G., 2002. Ultrastructural localization of tyrosine hydroxylase in human peripheral blood mononuclear cells: effect of stimulation with phytohaemagglutinin. Cell Tissue Res. 310, 297–304. https://doi.org/10.1007/s00441-002-0617-9.

Robinson, M.J., Ross, E.C., Franklin, K.B., 2011. The effect of propranolol dose and novelty of the reactivation procedure on the reconsolidation of a morphine place preference. Behav. Brain Res. 216, 281–284. https://doi.org/10.1016/j.bbr.2010.08.009.

Robinson, A.P., Harp, C.T., Noronha, A., Miller, S.D., 2014. The experimental autoimmune encephalomyelitis (EAE) model of MS: utility for understanding disease pathophysiology and treatment. Handb. Clin. Neurol. 122, 173–189. https://doi.org/10.1016/B978-0-444-52001-2.00008-X.

Rogers, P.R., Song, J., Gramaglia, I., Killeen, N., Croft, M., 2001. OX40 promotes Bcl-xL and Bcl-2 expression and is essential for long-term survival of CD4 T cells. Immunity 15, 445–455. https://doi.org/10.1016/S1074-7613(01)00191-1.

Rojo, A.I., Innamorato, N.G., Martin-Moreno, A.M., De Ceballos, M.L., Yamamoto, M., Cuadrado, A., 2010. Nrf2 regulates microglial dynamics and neuroinflammation in experimental Parkinson's disease. Glia 58, 588–598. https://doi.org/10.1002/glia.20947.

Rossi, A.G., McCutcheon, J.C., Roy, N., Chilvers, E.R., Haslett, C., Dransfield, I., 1998. Regulation of macrophage phagocytosis of apoptotic cells by cAMP. J. Immunol. 160, 3562–3568.

Roy, B., Rai, U., 2004. Dual mode of catecholamine action on splenic macrophage phagocytosis in wall lizard, Hemidactylus flaviviridis. Gen. Comp. Endocrinol. 136, 180–191. https://doi.org/10.1016/j.ygcen.2003.12.023.

Schetters, S.T.T., Gomez-Nicola, D., Garcia-Vallejo, J.J., Van Kooyk, Y., 2018. Neuroinflammation: microglia and T cells get ready to tango. Front. Immunol. 8, 1905. https://doi.org/10.3389/fimmu.2017.01905.

Semple, B.D., Kossmann, T., Morganti-Kossmann, M.C., 2010. Role of chemokines in CNS health and pathology: a focus on the CCL2/CCR2 and CXCL8/CXCR2 networks. J. Cereb. Blood Flow Metab. 30, 459–473. https://doi.org/10.1038/jcbfm.2009.240.

Shin, T., Ahn, M., Matsumoto, Y., 2012. Mechanism of experimental autoimmune encephalomyelitis in Lewis rats: recent insights from macrophages. Anat. Cell. Biol. 45, 141–148. https://doi.org/10.5115/acb.2012.45.3.141.

Sosa, R.A., Murphey, C., Ji, N., Cardona, A.E., Forsthuber, T.G., 2013. The kinetics of myelin antigen uptake by myeloid cells in the central nervous system during experimental autoimmune encephalomyelitis. J. Immunol. 191, 5848–5857. https://doi.org/10.4049/jimmunol.1300771.

Staedtke, V., Bai, R.Y., Kim, K., Darvas, M., Davila, M.L., Riggins, G.J., Rothman, P.B., Papadopoulos, N., Kinzler, K.W., Vogelstein, B., Zhou, S., 2018. Disruption of a self-amplifying catecholamine loop reduces cytokine release syndrome. Nature 564, 273–277. https://doi.org/10.1038/s41586-018-0774-y.

Stojić-Vukanić, Z., Kotur-Stevuljević, J., Nacka-Aleksić, M., Kosec, D., Vujnović, I., Pilipović, I., Dimitrijević, M., Leposavić, G., 2018. Sex bias in pathogenesis of autoimmune neuroinflammation: relevance for dimethyl fumarate immunomodulatory/anti-oxidant action. Mol. Neurobiol. 55, 3755–3774. https://doi.org/10.1007/s12035-017-0595-2.

Stritesky, G.L., Yeh, N., Kaplan, M.H., 2008. IL-23 promotes maintenance but not commitment to the Th17 lineage. J. Immunol. 181, 5948–5955. https://doi.org/10.4049/jimmunol.181.9.5948.

Tanaka, K.F., Kashima, H., Suzuki, H., Ono, K., Sawada, M., 2002. Existence of functional beta 1- and beta 2-adrenergic receptors on microglia. J. Neurosci. Res. 70, 232–237. https://doi.org/10.1002/jnr.10399.

Thompson, K.K., Tsirka, S.E., 2017. The diverse roles of microglia in the neurodegenerative aspects of central nervous system (CNS) autoimmunity. Int. J. Mol. Sci. 18, 504. https://doi.org/10.3390/ijms18030504.

Tomozawa, Y., Yabuuchi, K., Inoue, T., Satoh, M., 1995. Participation of cAMP and cAMP-dependent protein kinase in beta-adrenoceptor-mediated interleukin-1 beta mRNA induction in cultured microglia. Neurosci. Res. 22, 399–409. https://doi.org/10.1016/0168-0102(95)00922-G.

Vlcek, M., Penesova, A., Imrich, R., Meskova, M., Mravcova, M., Grunnerova, L., Garafova, A., Sivakova, M., Turcani, P., Kollar, B., Jezova, D., 2018. Autonomic nervous system response to stressors in newly diagnosed patients with multiple sclerosis. Cell. Mol. Neurobiol. 38, 363–370. https://doi.org/10.1007/s10571-017-0511-3.

Vujnović, I., Pilipović, I., Jasnić, N., Petrović, R., Blagojević, V., Arsenović-Ranin, N., Stojić-Vukanić, Z., Djordjević, J., Leposavić, G., 2019. Noradrenaline through β-adrenoceptor contributes to sexual dimorphism in primary CD4+ T-cell response in DA rat EAE model? Cell. Immunol. 336, 48–57. https://doi.org/10.1016/j.cellimm.2018.12.009.

Walker, F.R., Nilsson, M., Jones, K., 2013. Acute and chronic stress-induced disturbances of microglial plasticity, phenotype and function. Curr. Drug Targets 14, 1262–1276. https://doi.org/10.2174/13894501113149990208.

Wang, J., Li, J., Sheng, X., Zhao, H., Cao, X.D., Wang, Y.Q., Wu, G.C., 2010. Beta-adrenoceptor mediated surgery-induced production of pro-inflammatory cytokines in rat microglia cells. J. Neuroimmunol. 223, 77–83. https://doi.org/10.1016/j.jneuroim.2010.04.006.

Wang, L., Wang, R., Jin, M., Huang, Y., Liu, A., Qin, J., Chen, M., Wen, S., Pi, R., Shen, W., 2014. Carvedilol attenuates 6-hydroxydopamine-induced cell death in PC12 cells: involvement of Akt and Nrf2/ARE pathways. Neurochem. Res. 39, 1733–1740. https://doi.org/10.1007/s11064-014-1367-2.

Westlund, K.N., Bowker, R.M., Ziegler, M.G., Coulter, J.D., 1983. Noradrenergic projections to the spinal cord of the rat. Brain Res. 263, 15–31. https://doi.org/10.1016/0006-8993(83)91196-4.

White, S.R., Bhatnagar, R.K., Bardo, M.T., 1983. Norepinephrine depletion in the spinal cord gray matter of rats with experimental allergic encephalomyelitis. J. Neurochem. 40, 1771–1773. https://doi.org/10.1111/j.1471-4159.1983.tb08156.x.

Wilson, J., Higgins, D., Hutting, H., Serkova, N., Baird, C., Khailova, L., Queensland, K., Vu Tran, Z., Weitzel, L., Wischmeyer, P.E., 2013. Early propranolol treatment induces lung heme-oxygenase-1, attenuates metabolic dysfunction, and improves survival following experimental sepsis. Crit. Care 17, R195. https://doi.org/10.1186/cc12889.

Wohleb, E.S., Hanke, M.L., Corona, A.W., Powell, N.D., Stiner, L.M., Bailey, M.T., Nelson, R.J., Godbout, J.P., Sheridan, J.F., 2011. β-adrenergic receptor antagonism prevents anxiety-like behavior and microglial reactivity induced by repeated social defeat. J. Neurosci. 31, 6277–6288. https://doi.org/10.1523/JNEUROSCI.0450-11.2011.

Wohleb, E.S., Patterson, J.M., Sharma, V., Quan, N., Godbout, J.P., Sheridan, J.F., 2014. Knock down of interleukin-1 receptor type-1 on endothelial cells attenuated stress-induced neuroinflammation and prevented anxiety-like behavior. J. Neurosci. 34, 2583–2591. https://doi.org/10.1523/JNEUROSCI.3723-13.2014.

Wohleb, E.S., McKim, D.B., Sheridan, J.F., Godbout, J.P., 2015. Monocyte trafficking to the brain with stress and inflammation: a novel axis of immune-to-brain communication that influences mood and behavior. Front. Neurosci. 8, 447. https://doi.org/10.3389/fnins.2014.00447.

Wolf, Y., Yona, S., Kim, K.W., Jung, S., 2013. Microglia, seen from the CX3CR1 angle. Front. Cell. Neurosci. 7, 26. https://doi.org/10.3389/fncel.2013.00026.

Zeinstra, E., Wilczak, N., De Keyser, J., 2000. [3H]dihydroalprenolol binding to beta adrenergic receptors in multiple sclerosis brain. Neurosci. Lett. 289, 75–77. https://doi.org/10.1016/S0304-3940(00)01254-4.

Zhang, Z., Zhang, Z.Y., Schittenhelm, J., Wu, J., Meyermann, R., Schluesener, H.J., 2011. Parenchymal accumulation of CD163+ macrophages/microglia in multiple sclerosis brains. J. Neuroimmunol. 237, 73–79. https://doi.org/10.1016/j.jneuroim.2011.06.006.

Zoukos, Y., Leonard, J.P., Thomaides, T., Thompson, A.J., Cuzner, M.L., 1992. β-Adrenergic receptor density and function of peripheral blood mononuclear cells are increased in multiple sclerosis: a regulatory role for cortisol and interleukin-1. Ann. Neurol. 31, 657–662. https://doi.org/10.1002/ana.410310614.